Interaction between Katana bored pile foundation and ground beam in residential applications

Luke Simonelli
832797, lsimonelli@student.unimelb.edu.au

Chloe Pittle
832474, cpittle@student.unimelb.edu.au

Ashwynn Samrai
912752, asamrai@student.unimelb.edu.au

***Executive Summary**: This report investigated the interaction between the Katana screw pile and the soffit of a concrete ground beam in the construction of low-rise housing foundations. It aimed to determine the implications of the removal of a slab plate on manufacturing, site installation and structural detailing of the support concrete ground beam. This was achieved through a practical and theoretical investigation into the drive nut and concrete ground beam interaction. The removal of the slab plate saves materials and costs which add up to a significant amount over the application of hundreds of piles across a site. This would allow Katana Foundations to set a more competitive pricing that will benefit themselves and consumers. Moreover, the resulting reduction in steel reduces the embodied emissions of the screw pile system, an environmental benefit felt by the consumers and the wider community. The investigation compared the theoretical and experimental failure mechanisms at several locations along the beam to determine the extents of which the interaction satisfies the safe working limit of the screw pile without the slab plate. The Australian Standard's ability to predict punching shear failure of a waffle raft slab is also investigated.*

1 Introduction

Screw Piles are a piling method used for residential, mining, and light commercial applications that aim to achieve a high level of 'verticality' and soil penetration with minimal pre-drilling (Katana Foundations, 2021). Katana Foundations have provided such piles to the Australian and New Zealand residential sector since 2011, with 1.5 million installations across 26,000 jobs (Katana Foundations, 2021). Refer to Appendix A for standard drawings of screw piles. Bored pile and concrete ground beam interfaces are achieved through a removable slab plate, offering adjustable levels for the soffit of the ground beam and a larger surface area. This slab plate screws into the drive nut welded to the end of the pile, as illustrated in Figure 1, and the foundation (ground beam) sits upon this. The addition of the slab plate is not an insignificant additional cost, taking material and energy to produce, which adds up over the application of hundreds of piles across a large construction site. This research project investigates the interaction between the top of the pile cap, consisting of a drive nut, and soffit of the concrete ground beams to help determine if Katana Foundations can remove the slab plate, and what implications this will have on pile manufacturing, site installation and structural detailing of the support concrete ground beam. Thus, the project has ramifications for cost and material savings, which would allow Katana Foundation to set a more competitive pricing that will benefit themselves and consumers.

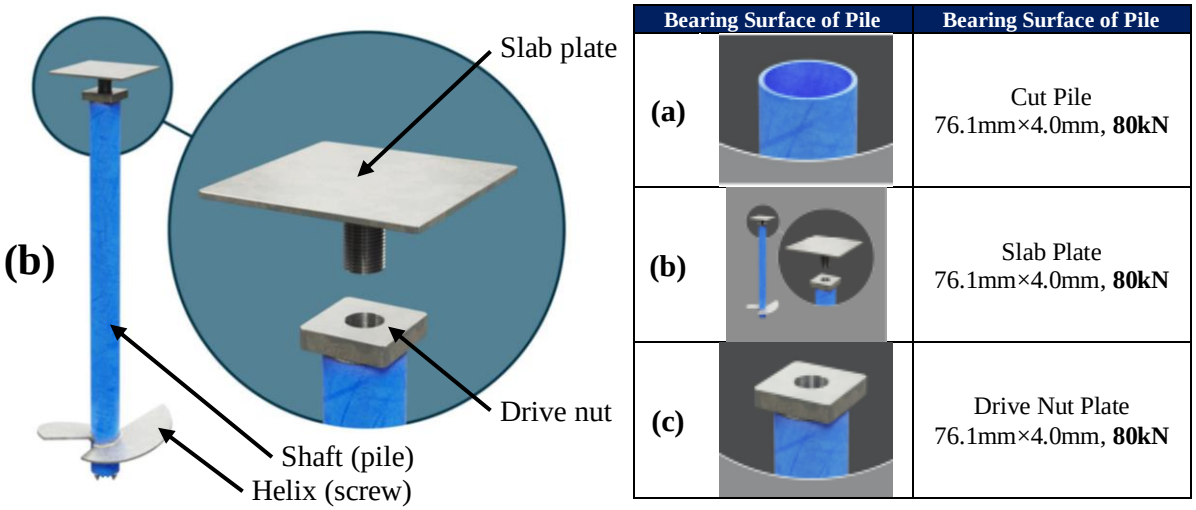

Figure 1. Katana screw pile with slab bearer plate (Katana Foundations, 2021)
(a) screw pile, (b) slab plate, (c) drive nut plate

The implications were determined through an investigation and a series of full-scale pile-beam interaction tests. Testing was conducted in the weakest typical conditions to satisfy end users. This was achieved by designing the ground beam per the minimum requirements of the relevant Australian Standards of 'Residential slab and footings (AS2970:2011)' (Standards Australia, 2011). By testing the drive nut interaction with the ground beam, the end of the screw pile without the slab plate shall be investigated to determine if it is required. The screw piles are to be tested at the desired and worst-case edge locations of the ground beam. The tests are used to deduce the site installation implications of removing the slab plate to achieve the safe working limit (SWL) of the screw pile (80 kN). Additionally, a cut pile, without the drive nut, shall be tested to determine the necessity of the drive nut material itself.

2 Literature Review

Traditional piles can be described as post-like foundation members which are driven into the ground to support a structure (Brittanica, 2022). Piles are used as they allow the building's load to be transferred to soil strata with sufficient bearing capacity and suitable settlement characteristics (Designing Buildings, 2022), allowing for construction in areas where the immediate ground conditions feature unfavourable characteristics. In comparison to traditional piles, screw piles are circular hollow steel sections with one or more helices welded to the shaft (Piletech, 2015) which allow for easy installation into the ground. The pile, which is typically made from high strength steel (Build, 2022) is then often capped at the top, with the house frame or foundations sitting atop this cap. It is imperative that the pile anchorage performs well without cracking the surrounding concrete as the pile-to-foundation connection is critical to the overall integrity of the system (Guner & Chiluwal, 2019).

The structural integrity of a piled foundation is also largely dependent on the design and strength of the reinforced concrete slab and ground beams. Generally residential foundations are cast in-situ as it allows for greater flexibility and adaptability in construction. However, it also introduces several factors which can affect the performance of the concrete foundation due to the variability of site conditions. Maintaining optimal environmental conditions during the curing of concrete is key to developing its desired strength. Excessively cold weather increases the setting time and slows the overall strength development of freshly placed concrete. If temperatures drop below 0°C, concrete curing effectively halts leading to reduced strength, durability and increase moisture permeability (Beall, 2001). Hot weather can demand a higher water content in the mix to achieve a desired slump and workability which can lead to an increased water to cement ratio thus resulting in loss of durability and strength (CCAA, 2017). In hot weather conditions, lower relative humidity can also accelerate loss of moisture. Decreased water content can lead to inadequate compaction, formation of cold joints during pouring, and excessive shrinking and cracking, all of which lead to strength development being compromised. Concrete that is not kept moist will only achieve about 50% of its design strength, whereas concrete that is kept moist for a full 28-day curing period will reach more than 125% of its design strength (Beall, 2001). As such, Australian Standard 'Specification and supply of concrete (AS1379:2007)' states at point of delivery concrete should have a temperature between 5-35°C (Standards Australia, 2007) to minimise impacts to the integrity of the concrete element. Comparatively precast concrete, which is cast using a mould or form and cured in a controlled environment, generally results in a higher standard finish and quality than in-situ elements (CCAA, 2006). As the curing conditions of the precast elements can be monitored, regulated, and accelerated as required, precast concrete is more likely to consistently meet its intended design performance.

This project focuses on the interaction between this mounting plate and the underside of the ground beam, specifically investigating the failure mechanisms of the slab when it is subjected to the reaction force from the top of the screw pile. Some key failure mechanisms which will be investigated in this review include failure in flexure and shear.

The first failure mechanism to be investigated is bending, or flexural failure. Bending failure occurs when the imposed load exceeds the flexural capacity of the of the materials of the beam (Hamakareem, 2022). Breaking this down further, there are three different types of flexural failure which can occur in a typical reinforced concrete beam. These include flexural tension failure, flexural compression failure, and balanced failure. Flexural tension failure occurs when the steel reinforcement in the beam yields first. This is followed by the 'crushing of concrete at compression side of the beam' (Hamakareem, 2022). This typically happens in situations where the beam is under-reinforced and can be characterised by large deflection. Flexural compression failure is the opposite of this; the concrete in compression is crushed first, followed by the 'yielding of steel at tension side' of the beam

(Hamakareem, 2022). This occurs when the beam is over-reinforced. Finally, balanced failure occurs when both flexural tension and flexural compression failure occur simultaneously. This explanation demonstrates the various ways in which a steel reinforced concrete section can fail in terms of bending. This information will help identify the failure method that has occurred during the testing of the concrete section for Katana foundations.

Turning next to shear failure, this occurs when 'the beam has a shear resistance lower than flexural strength and the shear force exceeds the shear capacity of different materials of the beam' (Hamakareem, 2022). This failure mechanism is 'characterized by shear sliding along a crack in the beam' (Paul, 2015) and typically occurs 'along a plane that is parallel to the direction of the force' (Hamakareem, 2022). The different types of shear failure include diagonal tension failure, shear compression failure, splitting shear and anchorage failure (Hamakareem, 2022), with most of these failures developing from cracks within the beam's cross-section. However, as described by Kotsovos (1987), most beams won't fail via shear failure, instead they will 'attain their flexural capacity' provided they have a sufficient shear span to depth ratio. This demonstrates that in most reinforced concrete, shear is an unlikely mode of failure if the concrete has been built to the correct specifications.

In instances of high pressure in a limited loading area concrete can also experience localised crushing. Crushing is caused by a concentrated external load when the applied stress over a loading area exceeds the confined compressive strength of the concrete. (Conforti, Tiberti, & Plizzari, 2016). High compressive stress will result in brittle failure causing cracks which under continued loading will propagate and lead to failure of the member. Concrete can be more susceptible to crushing when its strength is compromised due to factors during casting such as quality of concrete constituents, grading of aggregates, compaction, and water/cement ratio. For example, concrete samples with numerous voids and a poor aggregate interlock at likely to experience local crushing under high concentrated compressive loads.

When comparing the above failure methods, some methods of failure are preferable than others. As above, flexural tension failure and flexural compression failure exhibit very different properties during failure, being described as 'ductile failure' and 'brittle failure' respectively (Hamakareem, 2022). Like flexural compression failure, shear failure also falls into the category of brittle failure. Ductile failure is something that happens gradually, featuring 'slow propagation before the fracture occurs' (Corrosionpedia, 2020), comparatively brittle failure happens suddenly, and does not provide warning (Hamakareem, 2022). As such, in most applications' ductile failure, or flexural tension failure is preferred as brittle failure is described as 'brittle, dangerous failure' (Słowik, 2018). Evidently, ductile failure is the preferred option, as it fails gradually. The structure or element remains intact for some time during its failure, potentially allowing for preventative measures to be taken.

There have been previous publications and a project concerning Katana screw piles. A corrosive review of the Katana Screw Pile on Void Slab System by e3k predicts the basic Katana pile design to have a design life of 50 years or more in environments classified as 'non-aggressive' and 'mild' and special treatment is required to achieve this in environments classified 'moderate' or 'severe' (Hope, 2011). The Katana Screw Performance Guide discuses compression testing that determined the Safe Working Loads in stiff clay and dense sand of up to 80 kN for a 76.1 mm×4.0 mm, 250×8 Screw Pile (Katana Foundations, 2021). A previous project conducted by postgraduates from The University of Melbourne found the average yield torsional capacity experienced by the beams when driven into the ground is less than predicted at 80 % of the theoretical yield. The report went on to highlight that such discrepancy may be due to systematic laboratory impacts, which in this case were the effect of artificially aging test samples and prior yielding of connections (Sze, He, Di Cicco, & Luo, 2019).

3 Methodology

To thoroughly investigate the necessity of the slab plate, and implications of its removal, three different positions of the bored pile with the drive nut are to be tested. By doing so, a comparison can be made between the predicted (via calculations) and experimentally determined failure mechanisms. The data will then be used to extrapolate the failure force of screw pile locations along the beam. Thus, the acceptable distances from the center line to achieve the safe working load (SWL) of the screw pile (80 kN) or any other load requirement can be identified.

The first position to be tested (test 1) is the worst-case scenario at edge of the beam where eccentricity is at its highest. As such, it is expected to be the weakest compression bearing position. The second position to be tested (test 2) is in the center of the ground beam's step, which is the ideal and recommended location, experiencing no eccentricity. While the screw piles are meant to be positioned at this location, it is understood that there is much variation in residential construction. The third position to be tested (test 3) is directly between the first and second position to help describe the relationship between displacement from center line and failure.

An additional test (test 4), on the request of Katana Foundations, will be used to determine if the drive nut is required in ideal conditions. The cut pile will be loaded in the same position as the second test to determine if the drive nut can be removed, generating additional savings.

3.1 Beam Design

To satisfy users confidence in the report's findings, testing is to be conducted under the minimum requirements. Thus, the weakest typical real-world conditions will be replicated in laboratory testing. To achieve this, a waffle raft (see Figure 2) with the minimal allowable concrete grade (20MPa) and reinforcement (SL72 slab mesh and L8TM3 trench mesh) are to be adopted for testing conditions. The raft is to be designed in accordance with the relevant requirements of 'Residential slab and footings (AS 2870-2011)' (Standards Australia, 2011). Refer to Dwg. 1 in Appendix B for the ground beam detailed drawings. The beam is to be 2000 mm in length to prevent failure in flexure and explore the failure mechanism generated by the slab plate removal (explained later under Flexural failure). It should be noted, while these are the minimum requirements, they can only to be adopted in the best ground conditions. Typically, a higher strength concrete, larger reinforcement, and deeper beam is used, making laboratory results on the more conservative side.

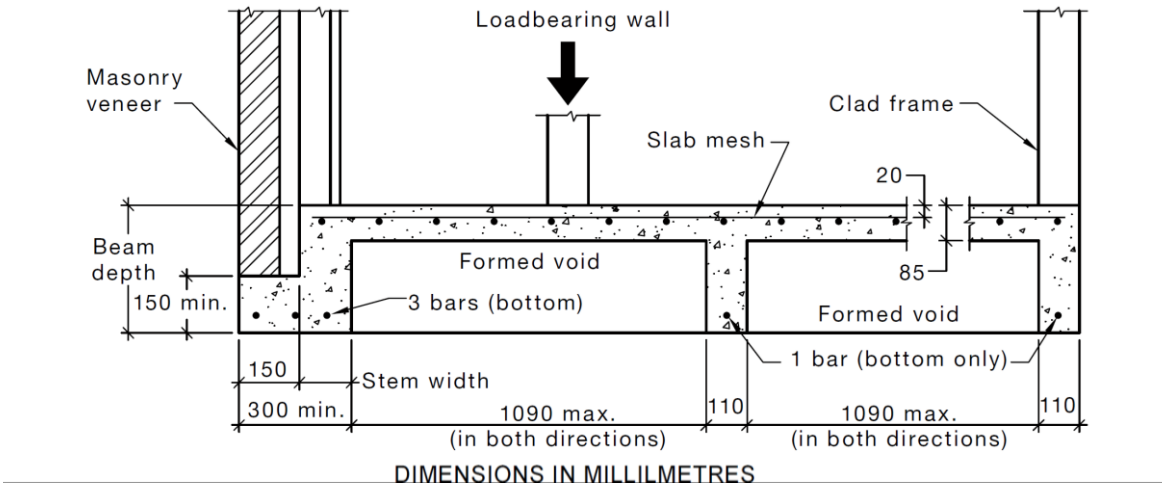

Figure 2. Waffle raft (Standards Australia, 2011)

3.2 Beam Fabrication

The concrete formwork is to be put together in such a way can be disassembled to remove the cast concrete beam and then re-assembled for the casting of the next beam. The top surface of the formwork was left exposed (open step) to ensure no voids form. Timber bracing and clamps are to be used to reinforce the formwork to prevent warping under the weight of concrete.

The concrete mixture needs to be relatively low slump due to the open face of the step in the formwork and have a fast-curing time (achieve 20 MPa in 2-weeks) due to the number of beams to be cast. The concrete mixture summarised in Table 1 satisfies these requirements.

Table 1. Concrete mixture

Materials	Water	Cement	Coarse aggregate (14 mm)	Fine aggregate (sand)	Total
for 1m^3 in kg	210	344	1300	558	2412

The curing of the concrete beam is to be monitored by concrete cylinder testing. 2 test cylinders are to be poured the same day as the beams. The concrete strength is to be taken 7 days and 14 days (testing day) from the pour date, to give an idea of the curing rate and strength at testing. This information will be used to adjust the recorded data to represent the desired 20 MPa concrete strength conditions. Due to the limited capacity of the concrete mixer (90 L) the concrete with be mixed in three batches. To investigate variability between batches, strength test cylinders are to be taken, and analysed, from each batch during the last beam pour. To prevent voids forming in the ground beam or test cylinders they are to be vibrated during pours. Exposed surfaces of cement are to be smoothed to ensure evenly distributed loading around the restraint and through the screw pile interaction.

3.2.1 Lifting requirements

The 401kg concrete beam will require lifting lugs cast into the beam to safely demold and maneuver the beam through crane operations from two lifting points. The lifting points are critical for safe lifts must be such that tipping, and pullout does not occur, and the moments are balanced during lifts. The lifting requirements must satisfy the requirements of ‘Prefabricated concrete elements - General requirements (AS3850.1:2015/Amdt 1:2019)’ (Standards Australia, 2019). The lifting points are to be at the vertical centroid of the beam’s cross section to prevent overturning during lifts. Furthermore, the points must balance the moment experienced during a lift to prevent cracking. Thus, the lifting locations are proposed as shown in Figure 3. Refer to Appendix C for calculations.

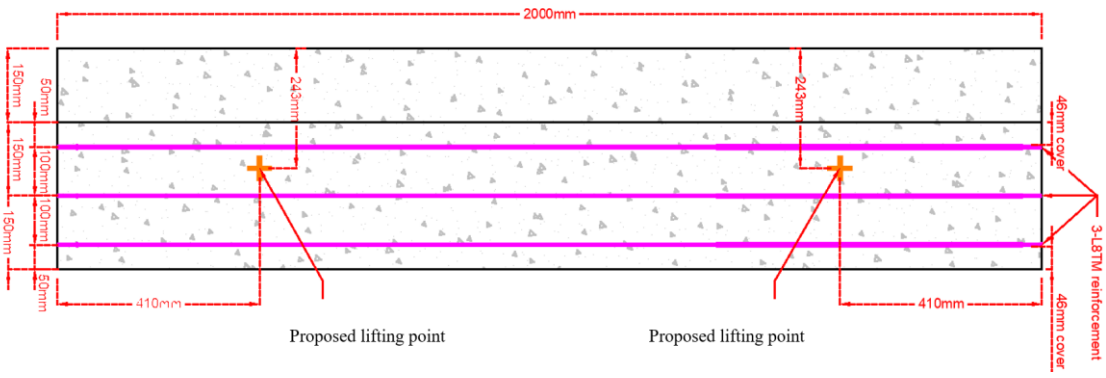

Figure 3. Proposed lifting locations (plan view)

To perform the concrete beam lift recessed 45 mm 1.3 t rated *SwiftLift™ Foot Anchors* are to be cast into the proposed lifting locations for use with an adequately rated lifting clutch. The capacity of these is checked for use at the proposed location and found to be adequate to perform the required beam lifts without concrete breakout failure occurring (refer to Appendix D for specification and calculations).

3.2.2 Casting procedure

The concrete beam is cast in the following steps, illustrated in Figure 4:

1. The materials for the concrete mix are weighed out and divided into 3 batches
2. The formwork and mould are oiled with a form release agent to prevent bonding with the forms, and slab mesh fitted into the formwork on reinforcement chairs.
3. The first batch of concrete is mixed. First the sand and aggregate are mixed in the cement mixer to ensure an even distribution of fine and coarse aggregate. The cement is then added, and mixing resumed while the water is slowly added, ensuring no clumping occurs.
4. Once all the water is added and concrete is adequately mixed, it is poured into the formwork.
5. A cement vibrator is used to draw out air and water bubbles that form voids within the mixture to.
6. The next batch is mixed, poured and vibrated the same way.
7. The trench mesh and lifting lugs are hung into position using wire before the final batch of concrete is mixed.
8. The final batch is poured into two concrete test cylinder moulds and the formwork, which are all vibrated to remove voids.
9. All exposed surfaces are then smoothed over before a tarp is placed over the form to limit any external environmental influence.
10. After 7-days, the beam and test cylinders are demoulded. Strength test 1 of the cylinders.
11. After 14-days, strength test the remain cylinder. If close to or greater than 20 MPa, preform test. Otherwise, delay testing a day or two to allow the beam to reach closer to the desired strength.

Step 0 – (Pre-casting) fabricate deformable concrete mould

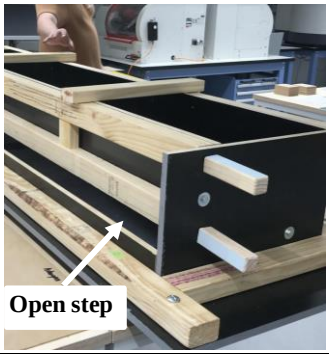

Step 1 – Weigh out materials and oil form

Step 2 – Place slab mesh and chairs within form

Step 3 – Mix aggregate and sand

Step 4 – Mix in cement and progressively add water

Step 5 – Pour mix into form and vibrate

Step 6 – Repeat steps 3 to 5 for next batch

Step 7 – Hang trench mesh and lifting lugs

Step 8 – Repeat steps 3 to 5 for final batch but include test cylinders

Step 9 – Smooth exposed surfaces and cover

Step 10 – (7 days later) demould beam and cylinders. Perform a strength test.

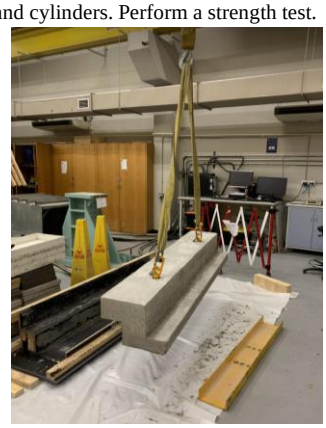

Step 11 – (14 days later) Perform strength test and experimental test (or delay).

Figure 4. Concrete casting

3.3 Test Setup

To efficiently re-create the ground beam and pile interaction under laboratory conditions, the set-up is to be flipped upside down. In residential applications, a load, usually from the residential dwelling, is applied through the ground beam into the pile and crushable void former (formed void) to the ground, illustrated in Figure 5. Refer to Figure 6 for illustration in residential application. To recreate this system under laboratory conditions, the beam was flipped. This allowed the pile to be loaded through a 500 kN actuator into the centre of a sufficient section of the ground beam, at various offset positions from the centre line towards the outer edge, illustrated in Figure 7, Figure 8 and Figure 9. The additional support provided by the masonry veneer were not considered despite their ability to reduce the moment induced by eccentricity, as they are not designed specifically to do so.

To simulate the residential application and prevent the ground beam from tipping under the applied load it must be restrained. A 200 UB 29.8 or larger steel beam, that fits neatly on the lip of the ground beam, is adequate to restrain the concrete ground beam (<5mm deflection) during testing (determined in Appendix E). The restraint will be bolted via steel sections to the ground, at its ends and centre (refer to Dwg. 2 in Appendix B for the experimental set-up detailed drawings).

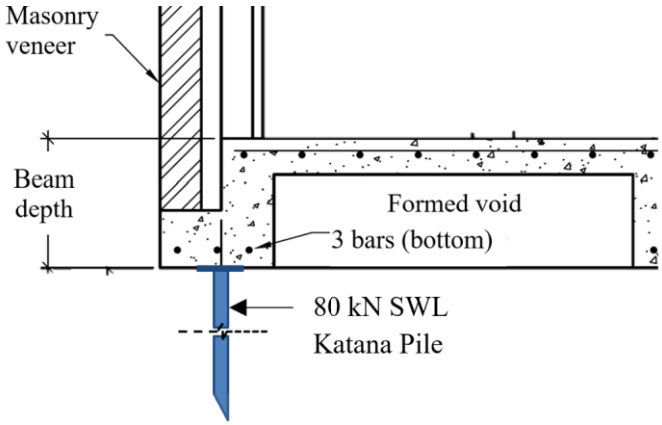

Figure 5. Residential application set-up of ground beam – screw pile interaction

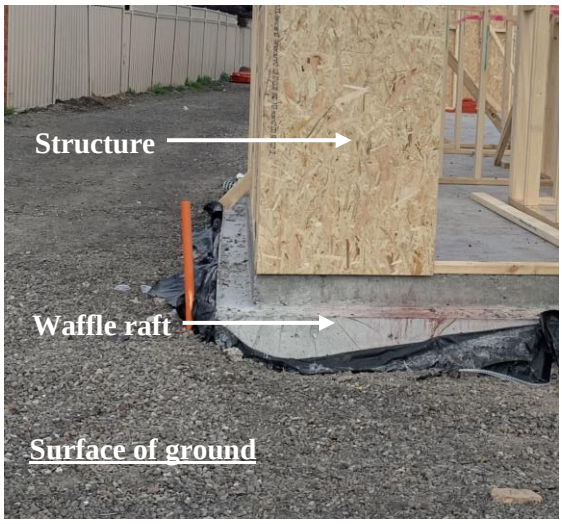

Waffle raft (ground beam)

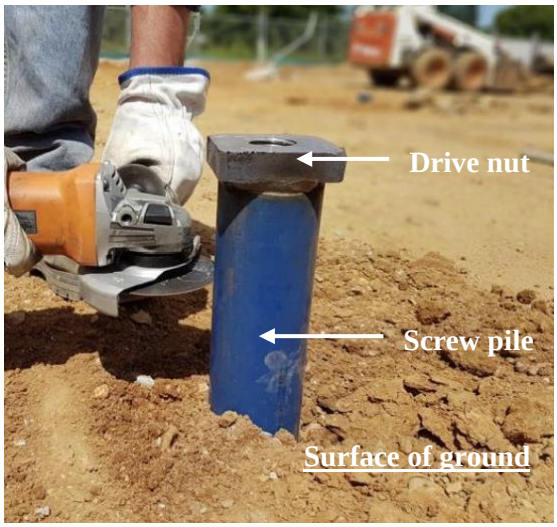

Screw pile with drive nut

Figure 6. Residential application of waffle raft and screw pile

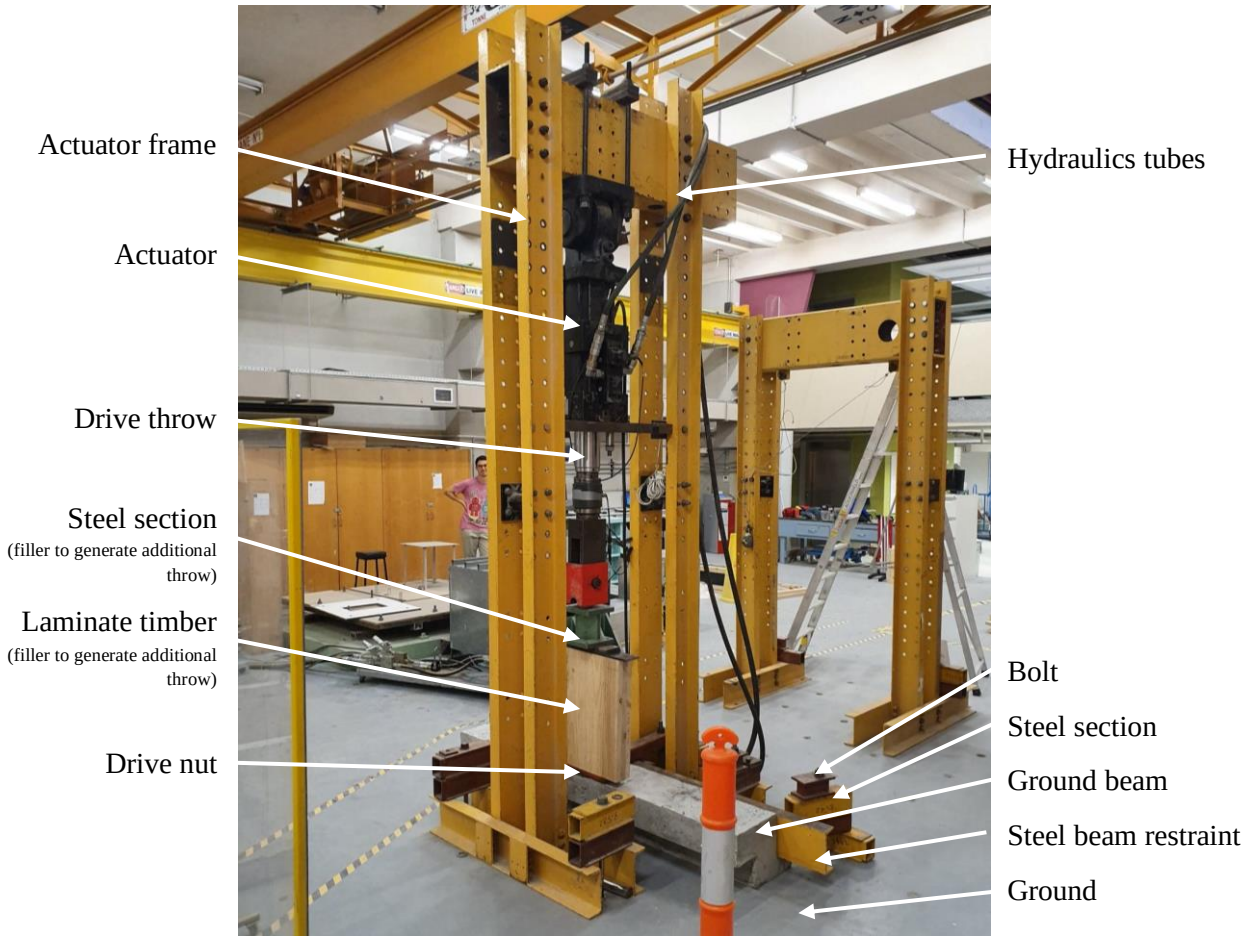

Figure 7. Experimental actuator set-up

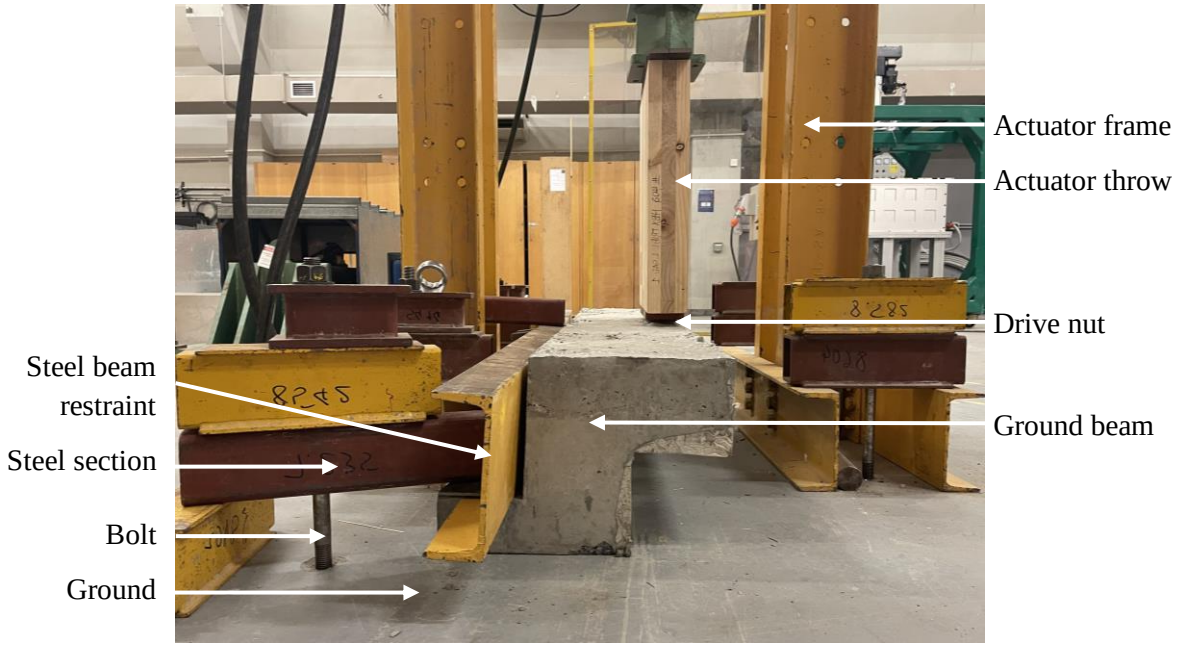

Figure 8. Experimental beam set-up

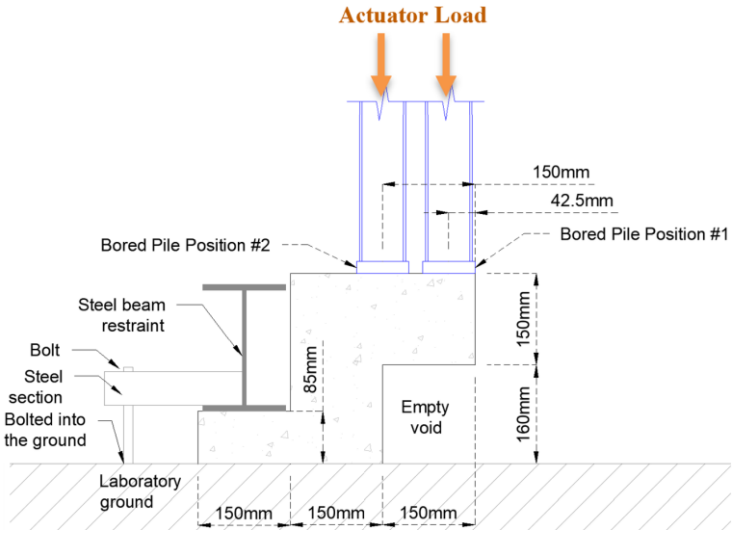

Figure 9. Experimental set-up diagram

3.4 Testing Procedure

First the theoretical failure of each of the tests is to be determined using the Australian Standards. Punching shear, local crushing and flexural compression are the expected failure mechanisms from the screw pile and waffle raft interactions. Calculations of potential punching shear and flexural compression failure mechanisms will identify the theoretical ultimate strength.

14-days after a beam is cast, it is ready for testing. The concrete beam is placed in the actuator, with the drive nut and beam positioned to perform the desired test. Once set-up, the actuator will be loaded, graphing the axial displacement and axial force. The test will be conducted until the ultimate strength is reached and failure occurs, or the actuators capacity is reached (500 kN).

The data is to be adjusted to accurately represent the minimum 20 MPa concrete strength conditions (*CD*) as variability in the actual concrete strengths during tests is expected due to environmental factors that influence concrete curing (i.e. temperature, moisture, etc.). This is achieved through by applying (1), under the assumption that the theoretical relationship between the concrete strength and ultimate strength (*US*) failure holds. To perform this calculation the concrete *strength at test day* is determined by testing the last test cylinder.

$$CD = \frac{theoretical\ US\ at\ 20\ MPa}{theoretical\ US\ at\ strength\ recorded\ on\ test\ day} \times actual\ US \quad (1)$$

The corrected data and theoretical failure is analysed to infer the practical and theoretical requirements of removing the slab plate and drive nut. A comparison between the actual and theoretical results determines the relationships between these and how conservative the theoretical calculations are. Thus, the screw piles allowable proximity to the edge of the beam without a slab plate can be determined.

4 Results and Discussion

4.1 Theoretical Failure Mechanism

Punching shear, local crushing and flexural compression are the expected failure mechanisms from the screw pile and waffle raft interactions. Calculations of the potential punching shear and flexural compression failure mechanisms identify the theoretical ultimate strength. It is important to note that, unlike the punching shear and local crushing failure mechanisms, the removal of the slab plate which reduces area of concrete-pile interface and thus average shear perimeter is not expected to impact the flexural strength.

4.1.1 Punching shear failure

The applied loads at which punching shear failure occurs are to be determined as per the specifications of 'Concrete structures (AS3600:2018)' (Standards Australia, 2018). When the moment (M_v^*) is zero, the ultimate shear strength (V_{uo}) is given by (2), and when M_v^* is not zero, V_u is given by (3) .

$$V_{uo} = ud_{om}(f_{cv} + 3\sigma_{cp})$$

where $f_{cv} = 0.17\left(1 + \frac{2}{\beta_h}\right)\sqrt{f_c'} \leq 0.34\sqrt{f_c'}$ as per *cl. 9.3.3(1)* of (AS 3600:2018) (2)

$$V_u = V_{uo}/[1.0 + uM_v^*/(8V^* ad_{om})]$$ as per *cl. 9.3.4(1)* of (AS 3600:2018) (3)

where u is length of critical shear perimeter (refer to Figure 10 and Figure 12),

d_{om} is mean value d_o of around critical shear perimeter (150 mm),

d_o is the distance from the extreme compressive fibre of the concrete to the centroid of the outermost layer of tensile reinforcemnt or tends,

σ_{cp} is the average intensity of effective prestrees in concrete (0),

β_h is the ratio of longest overall dimension of effective loaded area, Y, to perpindilucar dimension, X

f_c' is the strength of concrete (20 MPA),

M_v^*/V^* is the lever arm,

and a is the dimension of the critcal shear perimeter measured parallel to the direction of M_v^* (refer to Figure 8 and Figure 10).

Figure 11 and Figure 12 illustrate adjustment of the shear perimeters and areas from a standard slab, per the Australian Standards (refer to Figure 10), indicated in orange, to the geometry of the ground beam, indicated in blue.

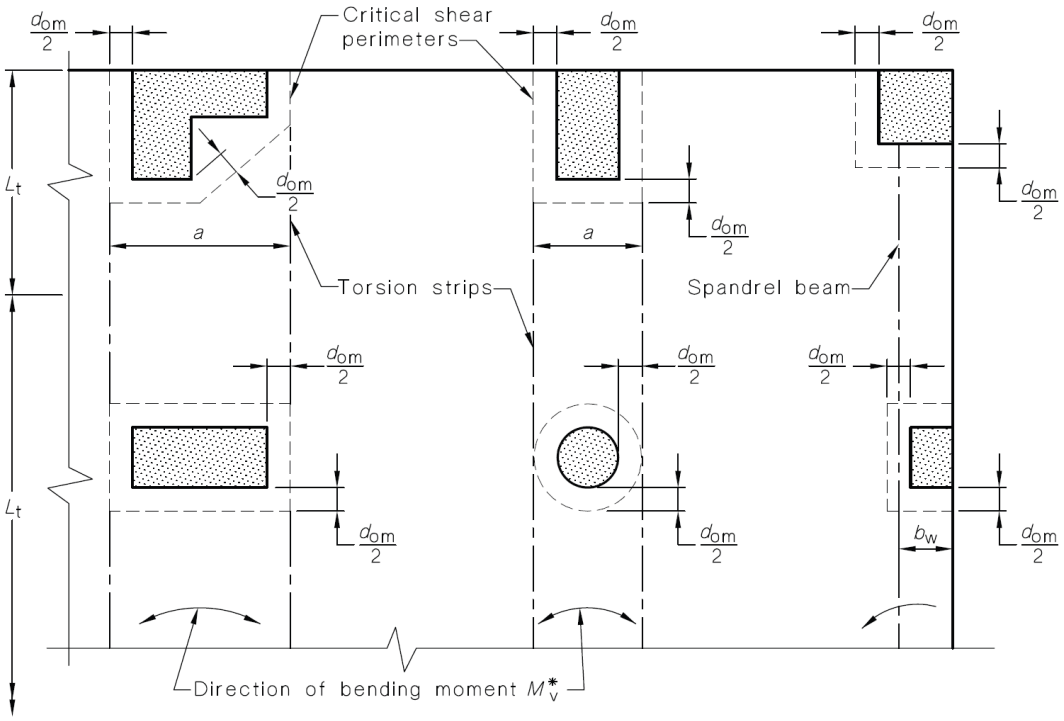

Figure 10. Torsional strips and spandrel beams (Standards Australia, 2018)

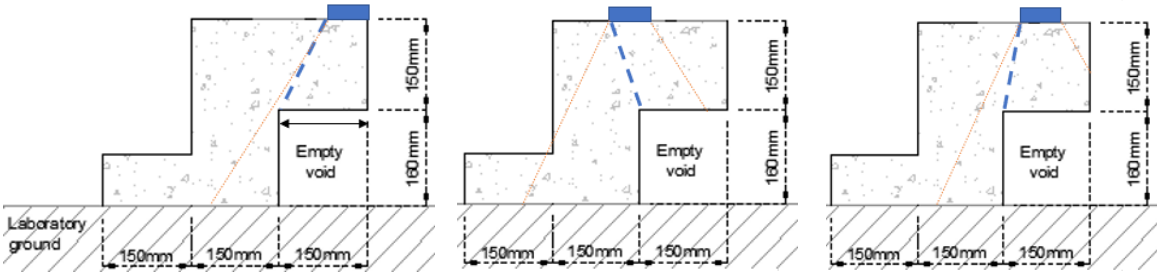

Position 1 **Position 2** **Position 3**

Figure 11. Critical shear plain – cross section

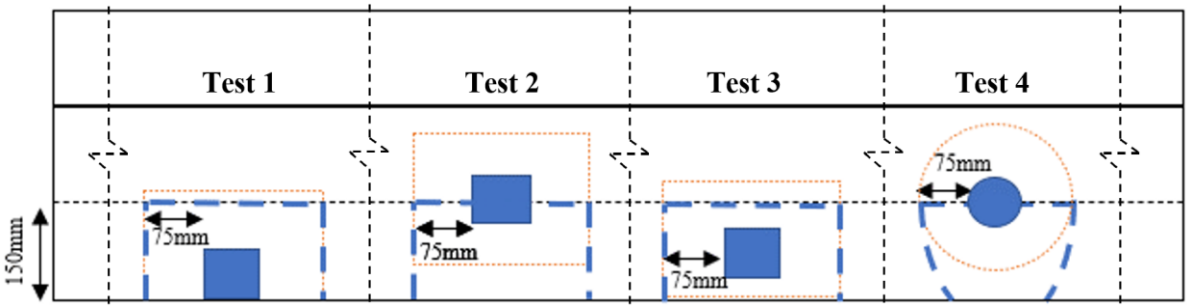

Figure 12. Critical shear plain – plan view

4.1.2 Flexural failure

It is expected that if flexural failure occurs it will be in the section emphasised in Figure 13 due to the applied force V^*. As the removal of the slab plate does not affect the flexure of the beam, the piles would be spaced regardless of the screw pile end to prevent this failure mechanism. Thus, as previously mentioned, the beam is to be an be adequate length so that flexural failure does not occur. For the flexural strength to be adequate, (4) must be satisfied with the compression and tension forces illustrated in Figure 14.

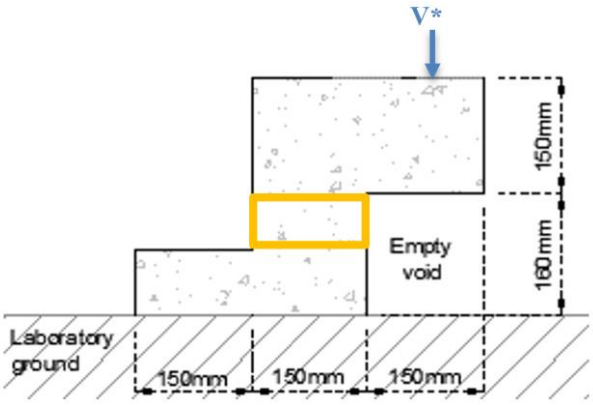

Figure 13. Bored Pile Diagram (flipped)

$$M^* < \phi M_{ub} \tag{4}$$

where $\phi M_{ub} = \phi C j_u = \phi(a_2 f_c' \gamma k_u db) j_u$

$= 18.97\ kNm$

where $\phi = 0.65$, as per *cl 3.1.3(1)* of (AS 3600:2018)

f_c' is the strength of concrete on compression (taken as the minimum allowable) (20 MPa),

a_2 is the coefficient for uniform compressive stress block of concrete, given by (6), as per *cl 3.1.3(2)* of (AS 3600:2018)

γ is the ratio of the depth of the assumed rectangular compressive stress block to k_ud, given by (7), (5)

k_u is neutral axis parameter, the ratio of the depth to the neutral axis from the extreme compressive fibre to d, given by (8),

b is the length of the section (2000 mm[1])

j_u is given by (9), and

M^* is the moment determined by (10).

$$a_2 = 0.85 - 0.0015 f_c' = 0.82 \geq 0.67 \quad \text{as per } \textit{cl 3.1.3(1)} \text{ of (AS 3600:2018)} \tag{6}$$

$= 0.82,$

$$\gamma = 0.87 - 0.0025 f_c' \geq 0 \quad \text{as per } \textit{cl 3.1.3(2)} \text{ of (AS 3600:2018)} \tag{7}$$

[1] 2000 mm prevents the beam from failing in flexure and is the typical spacing according to the industry partner

$\gamma \quad = 0.82,$

$$k_u = \frac{f_t'}{f_c'} = 0.1 \qquad \text{as no reinforcement} \qquad (8)$$

$$j_u = d - 0.5\gamma k_u d = 102mm \qquad (9)$$

$$M^* = V^* d_l$$

where V^* is the applied axial force,
and d_l is the lever arm of the eccentric axial force of the screw pile to the center of the beam section shown in Figure 15. (10)

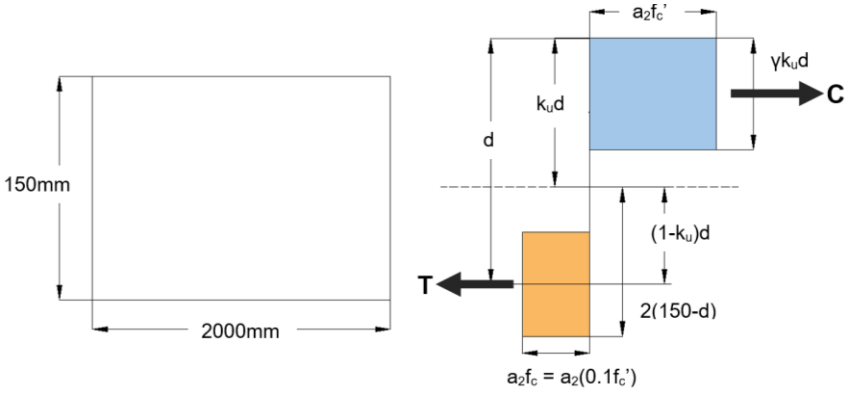

Figure 14. Compression and tension on failure area

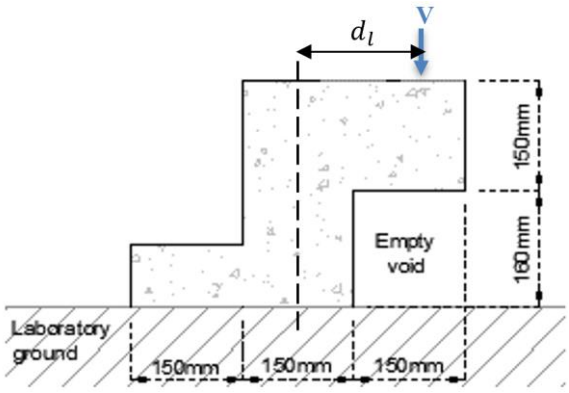

Figure 15. Bored Pile to Centre of the Concrete Beam

The concrete beam, with a length of 2000 mm between piles, is not expected to fail in flexure as $M^* < \phi M_{ub}$ (18.97 kNm) at the applied force at which punching shear failure is expected, as proven in Figure 16.

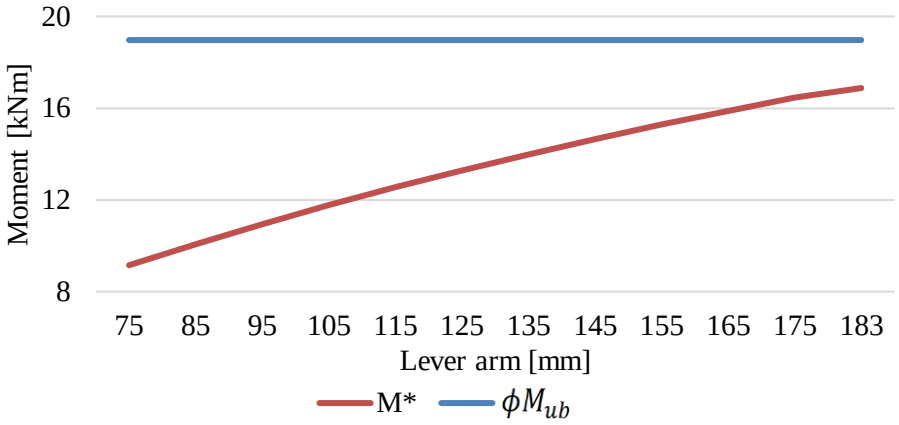

Figure 16. Moment capacity and design moment graphic

4.2 Observed Failure Mechanism

The data obtained from the actuator is plotted, ultimate strength standardised to 20 MPa concrete strength (refer to Appendix F for laboratory observations). Comparisons are then made between the theoretical and observed failure, the data of which is summarised in Table 2 and Figure 25.

Table 2. Test data summary

Test	Eccentricity[2] [mm]	f'_c [MPa]	Force at failure [kN]			Difference [%]
			Test data	Corrected data (20MPa)	Theoretical	
1	108	16.09	69.60	77.60	92.48	17.48
2	0	28.00	264.04	233.13	122.02	7.44
3	54	26.27	111.94	97.67	105.21	58.59
4	0	29.19	161.73	133.9	122.02	9.28

4.2.1 Test observations

The first test (test 1) positioned the drive nut at a maximum eccentricity of 107.5 mm offset from the beam centre. The beam was tested at 14 days maturity and recorded a concrete strength of 16.09 MPa which was averaged from two concrete cylinder samples. As the actuator loaded the beam the rate of loading was reduced to observe the failure mechanism in the beam more closely. The beam reached a yield force of 69.44 kN before experiencing punching shear failure (illustrated in Figure 17) at an ultimate force of 69.60 kN, as shown in Figure 18. No flexural cracks or other failure was observed prior to the shear failure.

As the strength of the beam was below the desired concrete strength for testing [20 MPa], the ultimate strength value was scaled to account for the reduced concrete strength. The scaled failure force of the beam for an equivalent beam of 20 MPa strength was determined to be 77.80 kN. The results of test 1 show that a pile with a drive nut attachment, which is installed at maximum eccentricity from the beam centre, does not have capacity to bear the SWL load of the pile and will fail in punching shear.

[2] From centreline of the ground beam's interaction surface

Diagonal view

Top view

Figure 17. Test 1 observed failure

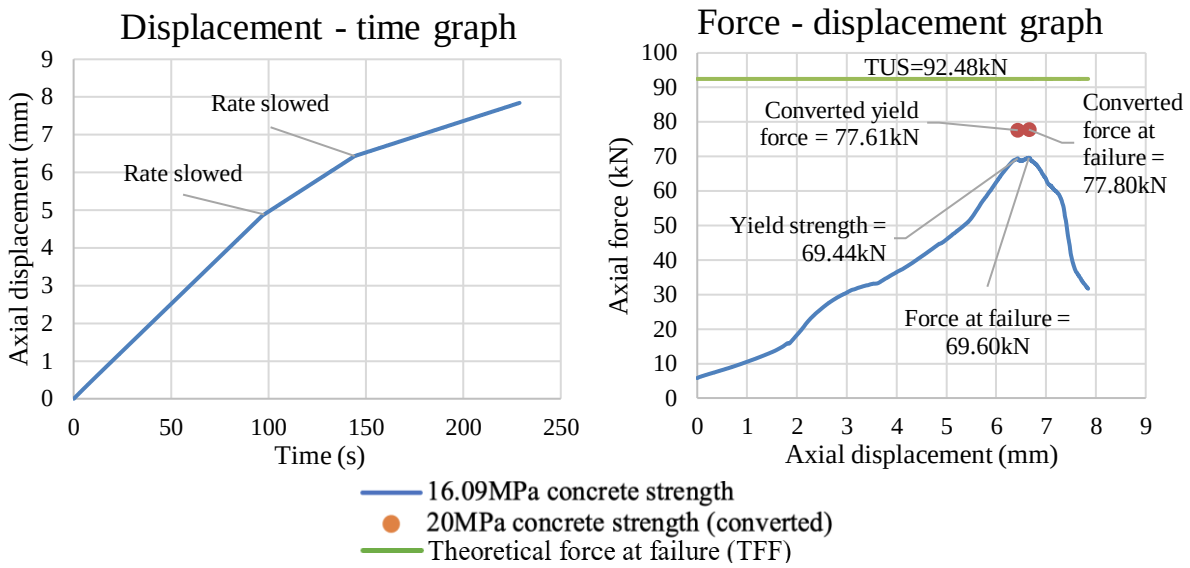

Figure 18. Test 1 (107.5mm) graphical data

In test 2, the drive nut was positioned in the centre of the top section of the beam, as shown in Figure 12 above. The cast was of a high quality, with a smooth finish on the top of the beam. In addition to this, the test cylinder tested above its expected value of 20 MPa after 14 days of curing, testing at 28.13 MPa. Once again, there was considerable variation between this value and the value generated by the Schmidt hammer.

The beam did not experience failure as the test was stopped prematurely. This was due to the limitation of the experimental setup which caused the force supplied by the actuator to peak at around 264 kN, as shown in Figure 20. The beam withstood a very high of compression force of and did not fail via punching shear as the other beams did. Flexural cracking occurred, propagating along the bottom of the beam as illustrated in Figure 19. In practise, the observed plane of a failure is unlikely. The stress experienced by the beam is inversely proportional to the width of the section. The ground beam in the experiment is part of a much larger slab section in practise, meaning the stress is spread over a much larger width, rendering flexural failure unlikely.

Accounting for the high strength of the test cylinders, the adjusted maximum force experienced by the beam of 223.13 kN is well above expectations. This proves that when the screw pile is centrally located, the drive nut provides a sufficient cap end to achieve a favourable strength and needs of the system (SWL [80 kN] < 223.13 kN).

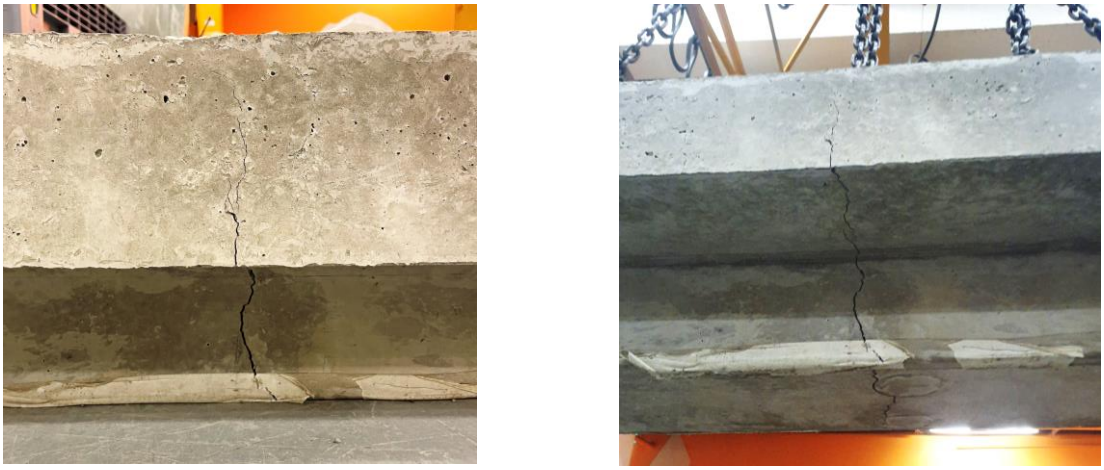

Front view **Bottom view**

Figure 19. Test 2 observed failure

‘

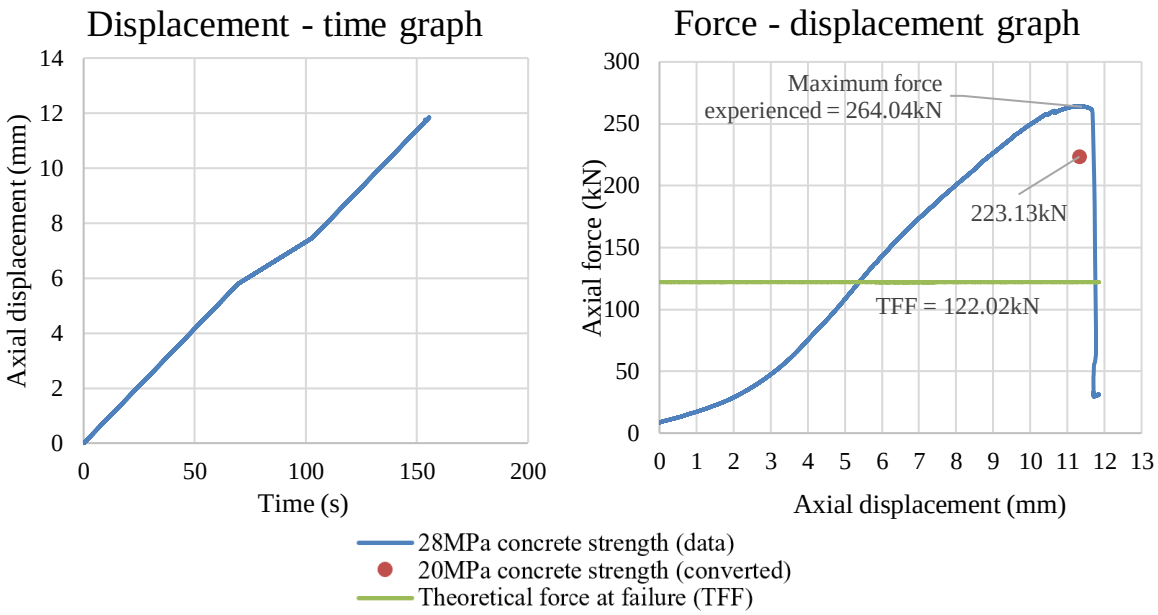

Figure 20. Test 2 (no eccentricity) graphical data

Similarly, to test 2, a vertical flexural crack was observed in test 3, explaining the local maximum on the force-displacement graph at 66.52 kN in Figure 22. The crack started forming around 60 kN in line with the axial load and slowly propagated up the beam. The loading rate was reduced here to carefully observe this crack. It is believed to be the result of voids between the aggregate, creating a weak point in the beam. The rate of the curve is similar before and after the local maximum, indicating the crack has had minimal impact on the beams ability to bear load. The influence of this is ignored as the

failure force is reached beyond this through punching shear failure (corrected data - 97.67 kN), illustrated in Figure 21. The observed failure indicates that the drive nut is a sufficient pile end at a 53.75 mm displacement from the center line (SWL [80 kN] < 97.67 kN).

Flexural crack – top lip **Diagonal view** **Top view**

Figure 21. Test 3 observed failure

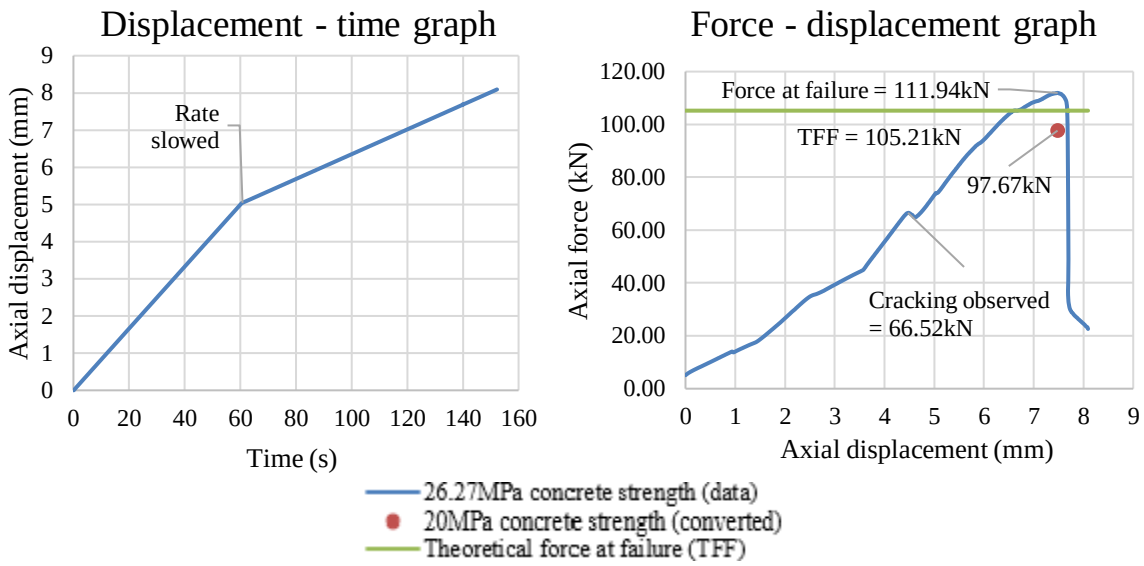

Figure 22. Test 3 (53.75mm) graphical data

In test 4 a cut pile was tested, positioned in a same location to test 2 (centre of the interaction surface of the beam). Once again, the cast was of good quality, however the test cylinders exhibited variable strength results – 16.89 MPa, 15.28 MPa and 11.05 MPa. These results delayed testing by a day, as the beam needed to be as close to 20 MPa as possible for more accurate results. Possible explanations for this variation are detailed later under ‘Systematic errors’.

The test exhibited a failure value of 161.73 kN, which was higher than expected as shown in Figure 24. Adjusting this value to what would be expected at a 20 MPa concrete beams gives 133.9 kN. This beam failed via punching shear, however it was observed to be a result of local crushing. It should also be noted that a flexural crack was observed on the underside of the beam after testing, however it was unclear when this formed or its impact. The local crushing caused the pile to re-position at a non-perpendicular angle to the beam, inducing the punching shear failure (illustrated in Figure 23). In

actual ground condition the pile would have been better restrained (by surrounding soil) and so this occurrence would be expected to occur at an even larger axial force. While failure occurred early, it was twice that of the SWL (80 kN) of the pile. Thus, a cut pile is an adequate screw pile system for use at the desired pile location at the centre of the interaction surface of the ground beam.

Front view – bottom lip **Diagonal view** **Top view**

Figure 23. Test 4 observed failure

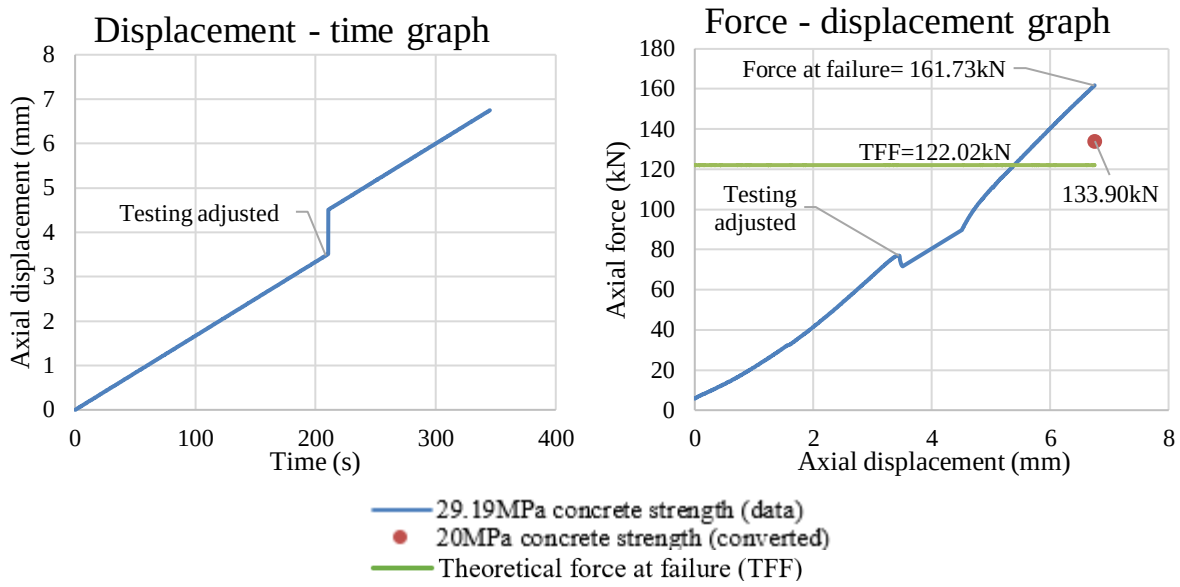

Figure 24. Test 4 (no eccentricity) graphical data

4.2.2 Discussion

Punching shear is the predominate failure mechanisms observed. Thus, while the applied method of punching shear failure calculation overestimates the failure force (see Figure 25), test 1 and 3 exbibit a similar factor (17.48 % and 7.44 %, respectively) of difference. Between these bored pile locations, a hyperbolic relationship would be expected between the failure force and eccentricity based on their relationship in the punching shear failure equations (2) and (3), with some additional factor of discrepancy to ensure it is conservative. Due to the declining failure force with increasing displacement from the observed data alone, it is deduced that the SWL of the pile will be reached up to a displacement of at least 53.75 mm (test 3). While there is a large increase in the failure force in the

ideal pile location of test 2, there is not sufficient data to model the failure mechanism transformation with the introduction of eccentricity. Additional testing is required to produce a more accurate model. While a factored model of predicted punching shear failure would be sufficient for design requirements, it would considerably underestimate failure force here leading to overdesign. This emphasises how much stronger the system is when screw piles are positioned in the correct location (test 2) with no moment inducing a punching shear.

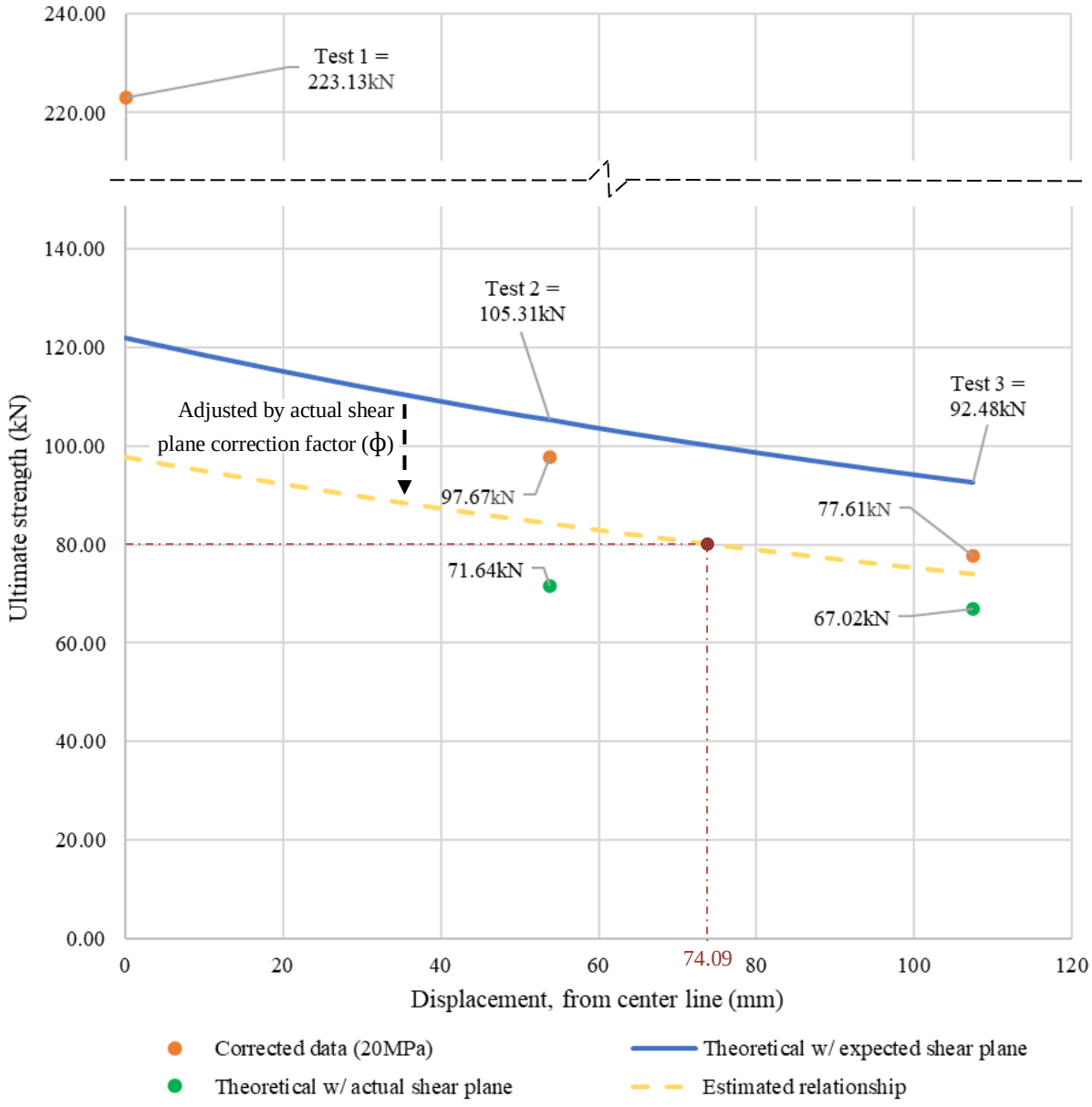

Figure 25. Failure force vs displacement (eccentricity) comparisons

The calculation of theoretical punching shear per the Australian Standard is expected to be conservative to ensure failure does not occur prematurely. This was not the case. A notable difference was observed between the predicted punching shear plane and what occurred in tests 1 and 3, illustrated Figure 26 and Figure 27. The ability of the Australian Standards to produce a conservative estimate of the punching shear failure in these beam conditions was determined by adjusting the shear plane inputs to that of the observed.

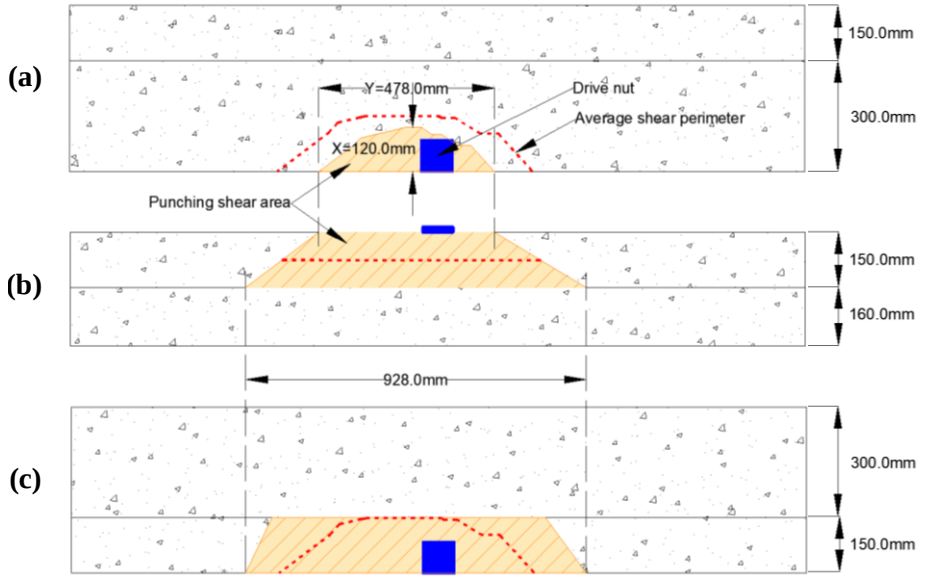

Figure 26. Test 1 actual shear plane
(a) plan view, (b) elevation view, (c) underside view

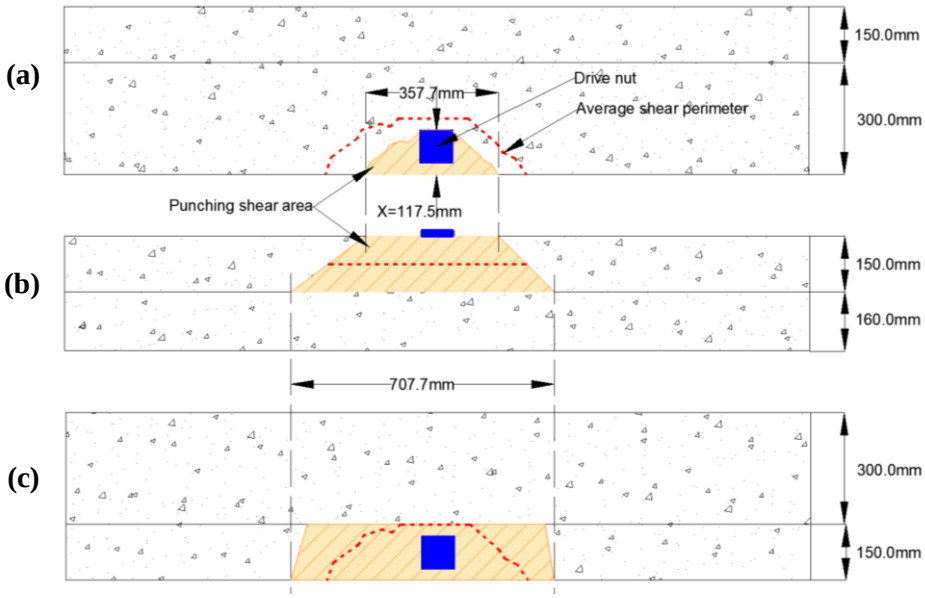

Figure 27. Test 3 actual shear plane
(a) plan view, (b) elevation view, (c) underside view

While the average shear perimeter was larger than predicted, increasing the strength, the increase in β_h ratio (defined in equation (3)) by treating the observed plane of shear on the surface of interaction as the effective loading area, had a stronger impact, reducing the strength (summarised in Table 3). The resulting punching shear calculation produces a conservative estimate of the failure observed, as illustrated in Figure 25. Thus, for the Australian Standards determination of punching shear failure to be applicable under these beam conditions, the shear plane must be adjusted from that described. The actual shear plane and failure cannot be accurately modelled from the two relevant data points experimentally obtained. Instead, a conservative estimation can be determined using the forementioned theoretical punching shear failure (illustrated in Figure 25) translated down by a conservative factor (greater than maximum discrepancy). An actual shear plane correction factor (ϕ)

of 0.8 is enough to conservatively predict the observed data (a ϕ = 0.6 will produce a model similarly conservative as the Australian Standard). Using this, the maximum displacement of a pile from the centre line to achieve the SWL of the screw pile (80 kN) is 74.09 mm. Furthermore, this translated model could be used to check the maximum displacement of a screw pile with a drive nut end subject to a load requirement, noting that there is a considerable underestimation of strength when to eccentricity approaches zero.

Table 3. Actual vs theoretical shear plane

Test	Theoretical μ [mm]	Observed μ [mm]	Theoretical β_h [Y/X]	Observed β_h [Y/X]	TFF with observed shear	μ difference [%]	TFF difference [%]
1	535	802	1.00	23.90	67.02kN	39.95	31.92
3	535	680	1.00	17.89	71.64kN	23.82	37.97

4.2.3 Theoretical assumptions

As the beams were tested at varying concrete strengths ranging from 16 to 28 MPa, it was assumed that the observed data could be adjusted, using equation (1), to determine the force at failure for an equivalent 20 MPa beam. This assumes the relationship between that the strength of the concrete and shear failure force, described by equations (2) and (3), holds in practise.

Several assumptions were made to determine a theoretical relationship between failure force of the beam and displacement of loading with respect to the observed shear failure planes. The shear failure planes shown in Figure 26 and Figure 27 were based on the measured failure paths for beams 1 and 3. The average shear area was assumed to occur at a depth of d/2 from the loading surface of the beam rather than the d/2 offset from the loaded area stipulated in AS3600:2018 (Standards Australia, 2018) (refer to Figure 10) which assumes a 1:1 failure plane. The spread of load through the section was based on the failure path observed on the front face of the section, shown in Figure 28. Furthermore, the shear plane on the surface of the interaction face of the beam is assumed to have acted as the effective loading area despite the actual loading area being smaller and symmetrical.

Figure 28. Measured front face of shear failure plane for test 3

4.2.4 Systematic errors

The experimental setup during test 2, which consisted of 3 I-beams strapped together underneath the actuator (shown in Figure 29), flexed considerably with the load veering off the vertical alignment. This unfortunately meant that the testing had to be paused and readjusted multiple times with steel beams placed to restrain the actuator. While this didn't necessarily have a prominent effect, as the testing location featured zero eccentricity, this issue needed to be mitigated in future tests. To rectify this issue, the steel I-beams were replaced by a block of cross-laminated timber, which mitigated deviation in the load path. An additional bolt from the actuator to the frame provided further restraint.

Flexure in system

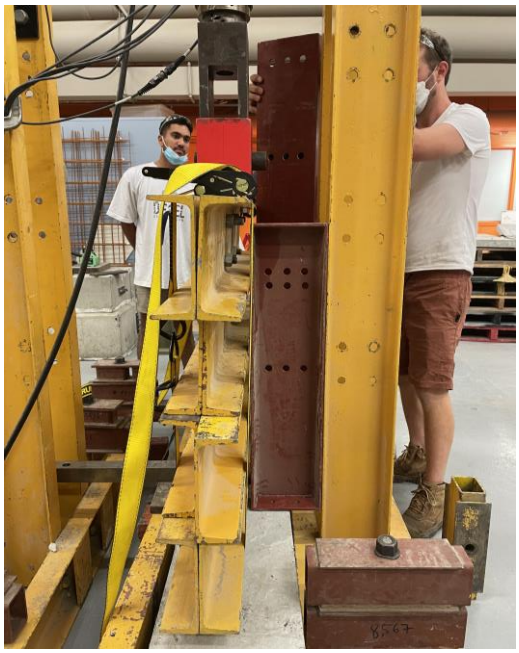

Temporary mitigation strategy

Figure 29. Test 2 setup – flexure in system and mitigation

The waffle raft was prefabricated while it is cast in-situ in most residential applications. Due to warping of the formwork inconsistencies were created between the ground beam and flat ground of the laboratory during testing, unlike in-situ casting. These inconsistences create another source of error in the replication of the residential application of screw piles and emphasise any imperfection in ground beam (i.e. cracks and voids). These imperfections are expected to be largely due to human error. This human error is the result of the limited experience beam castings, unlike the experience of contractors in practise. This may explain the unexpected flexural cracking observed during testing, leading to premature flexural failure during test 2.

Due to the actuator frame and the beam restraint, it was not possible to observe the formation and magnitude of flexural cracks in the bottom of the beam during testing. This occurred in multiple tests, and while the flexural strength of the beam is not expected to be the critical failure method, the presence of a crack likely reduced the beam's strength, causing premature failure and undervaluing the force of failure. This could have been overcome by positioning a camera in this location, however this camera would be at risk under the area loading and during testing.

A systematic error was introduced through testing of cylinders cast for beams 2 and 3 to determine concrete strength. Only one test cylinder was used to measure f_c' of the beam 2 and 3 prior to testing.

The reliability of the compressive strength values could have been improved by testing a minimum of two cylinders and deriving an average strength value as per the procedure recommended by 'Methods of testing concrete - Method 16: Determination of creep of concrete cylinders in compression (AS1012.16-1996:R2014)' (Standards Australia, 2014). The strength recorded for beam 1 was based on the average of two-cylinder test results and therefore is likely a more accurate estimate of compressive strength. However, best practice uses an average from three cylinder samples to estimate the f_c' of the beam as specified in AS1012.16-1996:R2014.

Due to laboratory constraints the beams manufactured for testing were cast with three to four separate batches of concrete. Variability within the concrete constituents such as minor variation in size, moisture, and presence of fines in each batch potentially led to strength variations within the beam thus the overall strength of the beam was not able to be accurately recorded. Casting the beam in separate batches may have also introduced strength inconsistencies within the beam such as cold joints. Testing shows that delays during concrete pours can preclude bonding between layers and create cold joints which result in significant tensile and shear strength variations (Nanayakkara et al, 2013). To limit impacts to the overall strength of the beam efforts were made to prevent formation of cold joints. Concrete constituents were pre-weighed prior to mixing of each batch to ensure lag time between pours was minimised. Additionally, during casting the beam was regularly vibrated with an immersion vibrator to mix the previously poured layer with the newly placed thus encouraging bonding between the layers and preventing cold joints. Visual inspection of the beam surface was undertaken prior to loading to ensure the surface was smooth and consistent.

At test 1, two test cylinders were poured per batch to compare concrete curing between batches. The cold weather during this period would explain the slower curing rate than expected. However, the growing difference between expected and average f_c' indicates that the cement may never achieve its desired strength (20 MPa), emphasized by the plateauing concrete strength – curing time curves in Figure 30. The other beams exceeded the desired strength at 14-days with the same concrete mixture indicating sources of variability between pours and curing, hence the 24 % coefficient of variation (CV) in beam strengths. This may be largely due to environmental factors (i.e.. temperature, humidity, etc.) that were not mitigated. To overcome the variation, that data was scale to the desired concrete strength using the relationship between punching shear strength and f'_c described in equations (2) and (3). The relative range drops significantly between batches (refer to Table 4), with a CV of 14 % at 7 days to 7 % at 14 days. This is believed to be due to minimal variation in the environment over the short period between batch mixtures. While the variability in strength of this beam between batches is relatively small it could have been larger for the other beams.

Table 4. Concrete curing data

Day	Batch 1 [MPa]	Batch 2 [MPa]	Batch 3 [MPa]	Average [MPa]	Std dev	CV [%]	Expected[3] [MPa]	Difference [%]
0	0	0	0	NA	NA	NA	0	NA
7	13.99	11.29	14.89	13.39	1.87	13.99	14.44	7.55
14	16.89	15.28	~~*11.05*~~[4]	16.09	1.14	7.08	20.00	21.67

[3] Typical strength of concrete is 65 % at 7 days and 90 % at 14 days (Mishra, 2014).

[4] Test cylinder visibly compromised with voids between aggregate – omitted from calculations with insufficient data to form model.

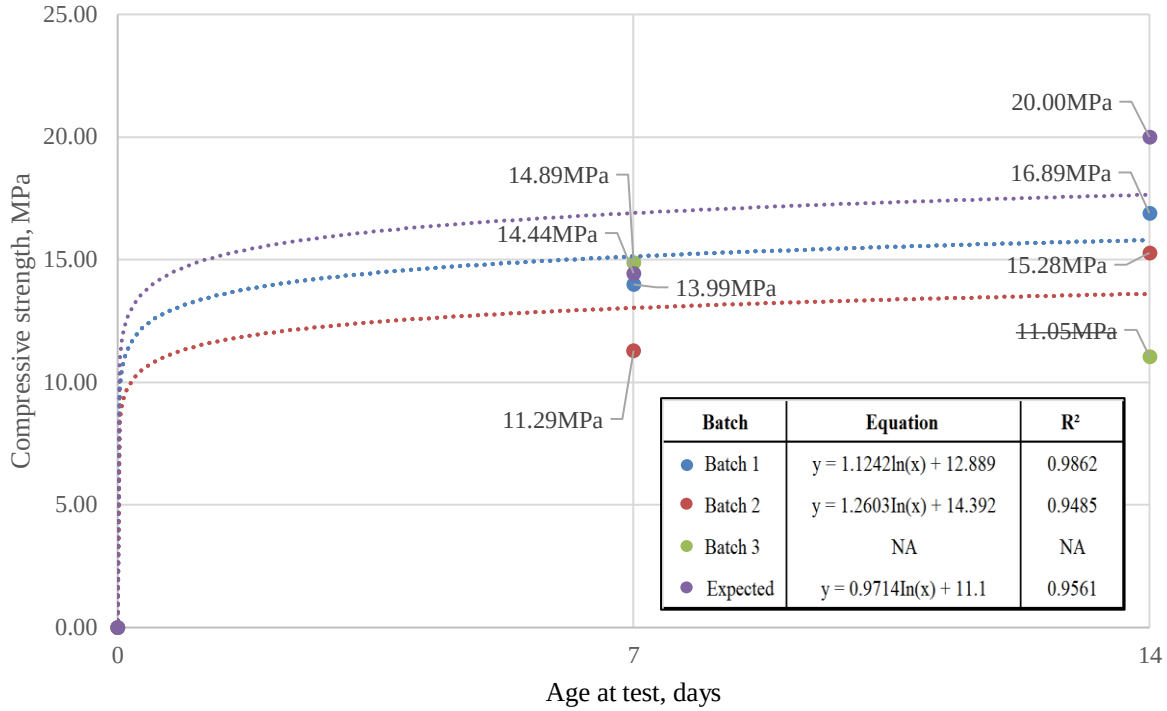

Figure 30. Concrete curing curve

4.3 Further analysis

To strengthen the results, further analysis is required to determine the eccentricity at which the failure mode transitions from flexural to punching shear. A sharp decline in failure force is expected with the introduction of eccentricity over 0 to 74.09 mm offset range. This would establish a more accurate measurement of the critical position at which punching shear failure occurs. Thus, a less conservative estimate of maximum displacement a drive nut can be positions can be determined, improving the constructability of the system.

Additional value would be provided by conducting further tests with the slab plate and other offered interaction attachments past the determined tolerance of the drive nut (74.09 to 107.5 mm). This would determine the attachments impact on the system's ability to bear the pile's safe working load. As the slab plate provides a larger bearing surface it may generate a larger critical shear perimeter, increasing the shear capacity of the beam (described by equations (2) and (3)). Confirmation of the contribution of the slab plate and other attachments on the shear strength of the system would allow users of the Katana foundation system to correct instances in which the piles are installed outside of the drive nuts recommended tolerance. Even further value could be provided by testing requirements of waffle raft (i.e. reinforcement, depth and type) to achieve to the SWL within this range.

Further testing into the impacts of long-term loading on the performance of foundation system would be provide further information on the long-term durability of the recommendations. Rapid construction and loading can cause deflection and cracking within the concrete members at an early age. Additionally, the effects of creep, the increased strain or deformation due to sustained loading, may result in stress redistributions within the beam which compromise the strength of the system. Understanding of the extent to which this can impact the ultimate strength of the beam and the point at which the failure mechanism changes from flexural to shear failure will add further value to the research.

The findings support the acceptable placement of an 80 kN rated screw pile. Katana Foundations offer a larger range of screw piles, rated 80, 100, 150 and 250 kN with the options of additional extensions. This goes beyond the maximum load capabilities of the tested ground beam (223.13 kN). At higher load ratings the requirements of the foundation (i.e. reinforcement, depth and type) will rise. Additional tests using ground beams replicating these requirements would be required to determine the acceptable placement tolerances of the drive nut at these higher load ratings.

5 Conclusions

An experimental investigation was conducted to investigate the interaction between a Katana screw pile and the soffit of a concrete ground beam. Testing was used to explore the implications of changing the position and end of bearing surface of the pile on the overall strength of the system and ability to meet the SWL of the screw pile. A total of 4 tests were conducted consisting of a cut pile test and 3 drive nut tests over a range of positions. From this a declining failure force with increasing eccentricity was observed, consistent with the hyperbolic relationship of punching shear as per the Australian Standards. Applying a conservative factor ($\phi = 0.8$) to the punching shear described in the Australian Standards was determined to provide a somewhat accurate estimate of observed punching shear, accounting for the geometrical differences of the waffle raft slab. Moreover, the Australian Standards were shown to provide a conservative estimate of punching shear when the actual shear plane is predicted/used. Thus, the drive nut should reach the screw piles SWL when the pile is located within a 74 mm tolerance from the centre of the ground beams interaction surface. Additionally, the drive nut can also be removed when the pile is located centrally, as the cut pile proved to be sufficient to achieve the SWL of the screw pile. Thus, environmental, and economic benefits can be achieved through the specified removal of slab plate and drive nut, saving material not necessary at these locations. The significantly higher force reached when the drive nut is centrally tested emphasises the sensitivity of the system to eccentric forces and thus the importance of achieving this in practise.

6 Acknowledgements

The completion of this project could not have been possible without the participation and assistance of many people whose name may not all be enumerated. We thank the project supervisors Dr. Phillip Christopher and Richard Nero (The University of Melbourne) for their continued support and input throughout the project along with the industry partner, Mark Armstrong (Katana Foundations). We also thank all the staff of Melbourne University's Francis Laboratory and Telstra Creator Space for their assistance, with a special thank you to Ray Furmston for undertaking many of the technical and labour-intensive aspects of the experimental set-up.

7 References

Beall, C. (2001). *Masonry and Concrete, 1st ed.* New York: McGrarw-Hill.

Brittanica. (2022). *Pile.* Retrieved from Brittanica: https://www.britannica.com/technology/pile-construction

Build. (2022). *Screw piers (or screw piles)*. Retrieved from Build: https://build.com.au/screw-piers-or-screw-piles

Cement Concrete & Aggregates Australia [CCAA]. (2006, May 1). *Guide to Off-form Concrete Finishes.* Retrieved from Cement Concrete & Aggregates Australia: https://www.ccaa.com.au/CCAA/Publications/Technical_Publications/Guides/CCAA/Public_Content/LISTS/Guides.aspx?hkey=a73e7f93-6887-4c45-a33b-e34cbb00bb2e

Cement Concrete & Aggregates Australia [CCAA]. (2017, August). *Hot-Weather Concreting.* Retrieved from Cement Concrete & Aggregates Australia: https://www.ccaa.com.au/CCAA/Public_Content/PUBLICATIONS/Technical_Publications/Datasheets/Hot_Weather_Concreting.aspx?WebsiteKey=4998d6ce-2791-4962-b1e2-6b717f54a8d3

Conforti, A., Tiberti, G., & Plizzari, G. A. (2016). Splitting and crushing failure in FRC elements subjected to a high concentrated load. *Composites Part B*, 82-92.

Corrosionpedia. (2020, August 7). *Ductile Failure*. Retrieved from Corrosionpedia: https://www.corrosionpedia.com/definition/6415/ductile-failure

Designing Buildings. (2022, March 11). *Pile foundations*. Retrieved from Designing Buildings: https://www.designingbuildings.co.uk/wiki/Pile_foundations

Guner, S., & Chiluwal, S. (2019). Effects of Detailing on the Behaviour of Helical Pile-to-Foundation Connections. *Proceedings of the XVI Pan-American Conference on Soil Mechanics and Geotechnical Engineering* (pp. 1002-1009). Toledo: IOS Press.

Hamakareem, M. I. (2022). *Failure Modes in Concrete Beams: Flexural and Shear Failure*. Retrieved from The Constructor: https://theconstructor.org/structural-engg/failure-modes-concrete-beams-flexural-shear/37752/

Hope, R. (2011). *Katana Screw Pile Corrosion Review on Void Slab Systems.* Brisbane: e3k.

Katana Foundations. (2018). *Katana Foundations.* Retrieved 02 30, 2022, from Foundation Systems Screw Piling: https://katanafoundations.com.au/foundation-systems/screw-piling/#1522715465513-2c04a5b4-2c1a

Katana Foundations. (2021, September 17). *Katana Screw Pile Performance Guide*. Retrieved from Katana Foundations: https://katanafoundations.com.au/wp-content/uploads/2021/09/17-9-2020-Katana-Screw-Pile-Performance-Guide.pdf

Kotsovos, M. (1987). Shear failure of reinforced concrete beams. *Engineering Structures, 9(1)*, 32-38.

Leviat. (2020, September). *Threaded Inserts Design Guide.* Retrieved from Ancon: https://www.ancon.com.au/products/precast-concrete-accessories/threaded-inserts

Mishra, G. (2014). *Compressive Strength of Concrete -Cube Test [PDF], Procedure, Results*. Retrieved from The Constructor: https://theconstructor.org/concrete/compressive-strength-concrete-cube-test/1561/

Paul, A. (2015, February 24). *Failure modes in beams: Types of Failure in Reinforced Concrete BEEAMS*. Retrieved from CivilDigital: https://civildigital.com/failure-modes-beams/

Perera, B., Piyasena, R., Premerathne, P., & Nanayakkara, S. (2013). Evaluation of Initial Setting Time of Fresh Concrete. *National Engineering Conference* (pp. 47-52). University of Moratuwa.

Piletech. (2015). *Practice Note Screw Piles: Guidelines for Design, Construction & Installation.* Institute of Professional Engineers New Zealand.

Ried. (2021, February). *Ried SwiftLift Foot Anchors.* Retrieved from Reid: https://reid.com.au/product/swiftlift-general-lifting

Słowik, M. (2018). The analysis of failure in concrete and reinforced concrete beams with different reinforcement ratio. *Archive Of Applied Mechanics, 89(5)*, 885-895.

STA Consulting Engineers. (2015, July 1). *Katana Foundations Product Guide.* Retrieved April 4, 2022, from Katana Foundations: https://katanafoundations.com.au/wp-content/uploads/2018/07/Product-Range-Katana-Pile-1-7-2015.pdf

Standards Australia. (2007). *Specification and supply of concrete (AS1379:2007).* Sydney: SAI Global.

Standards Australia. (2011). *Residential Slab and Footings (AS2970:2011).* Sydney: SAI Global.

Standards Australia. (2014). *Methods of testing concrete - Method 16: Determination of creep of concrete cylinders in compression (AS1012.16-1996:R2014).* SAI Global.

Standards Australia. (2018). *Concrete structures (AS3600:2018).* Sydney: SAI Global.

Standards Australia. (2019). *Prefabricated concrete elements - General requirements (AS3850.1:2015/Amdt 1:2019).* Sydney: SAI Global.

Sze, E., He, J., Di Cicco, S., & Luo, X. (2019). *Tube Torsional Capacity Investigation for Screw Piles.* Melbourne.

8 Appendices

8.1 Appendix A

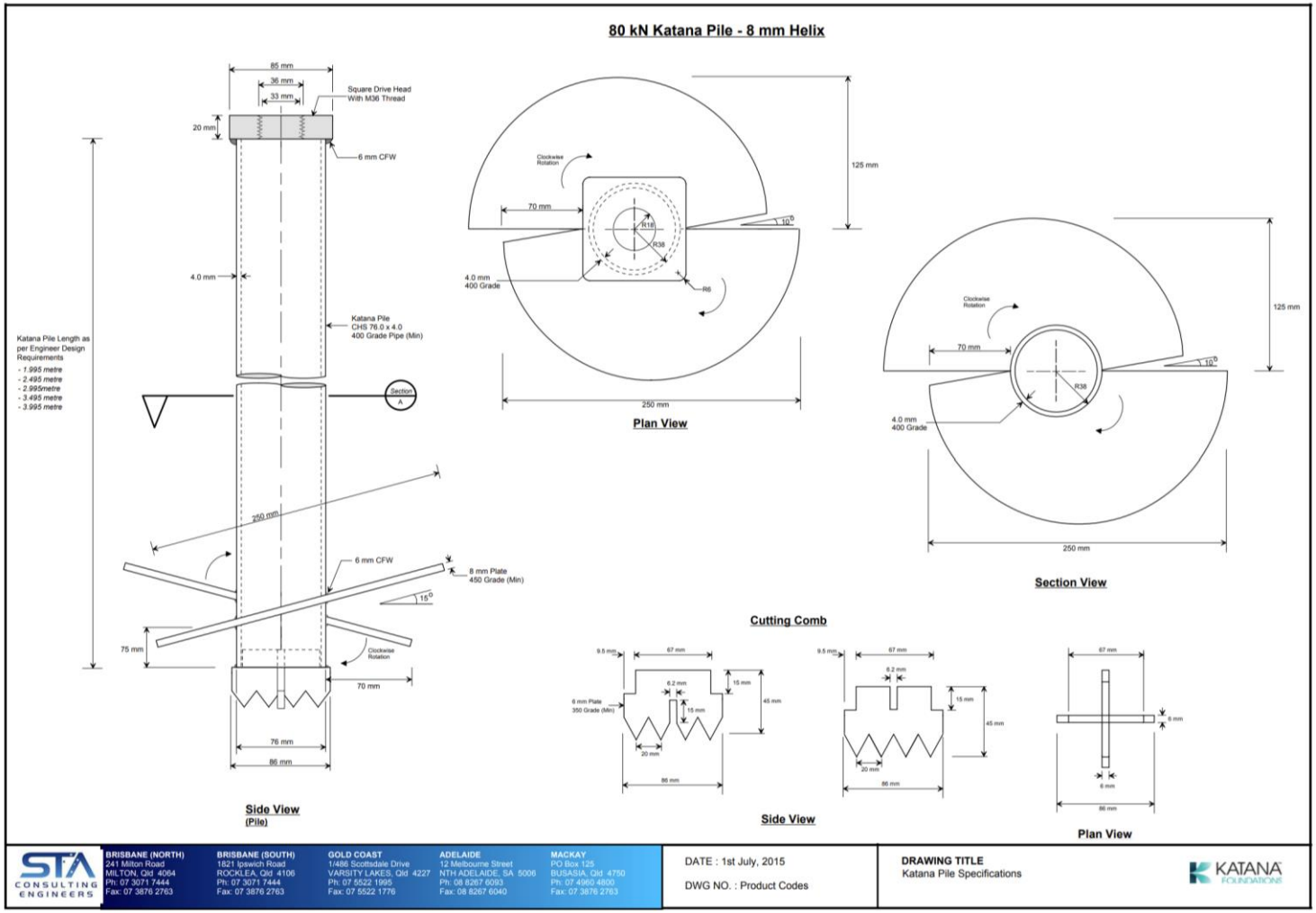

Figure 31. Katana Pile Specifications (STA Consulting Engineers, 2015)

8.2 Appendix B

Notes:

- Specifically require 20MPa grade concrete (not higher).
- 3-L8TM top reinforcement with a 40mm cover to the top surface of the beam.
- SL72 bottom reinforcement with a 20mm cover to the bottom surface and 40mm cover to the side surface of the beam, as detailed in '*Side View*'.
- Cast in recessed 45mm long 1.3t rated *SwiftLift™ Foot Anchors* (produce code: 1F045) in the proposed lifting points *or equivalent*.
- Fabricate standard concrete test blocks on the same day as reinforced concrete ground beams - for strength testing purposes.

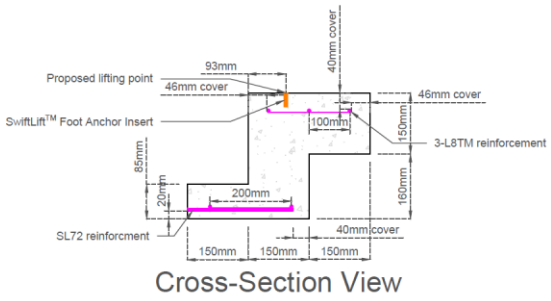

Cross-Section View

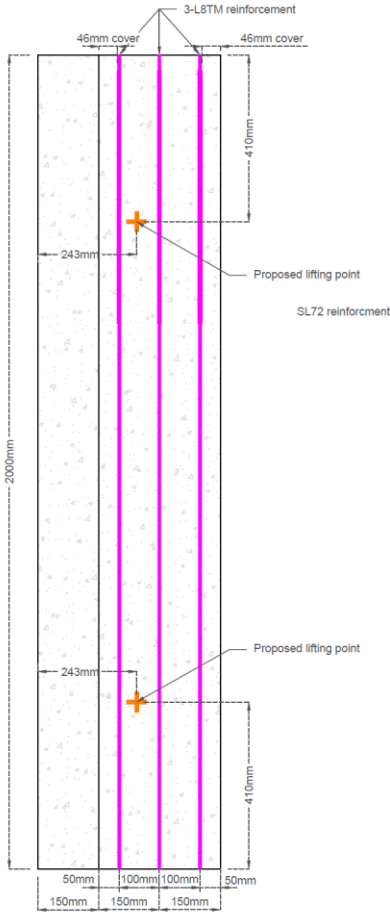

Plan View

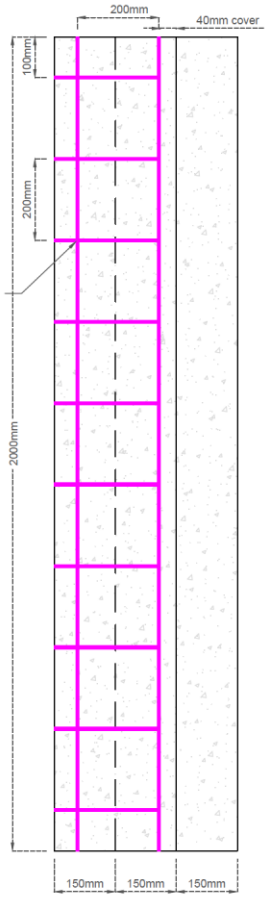

Bottom View

Dwg. 1	Detailed Drawings – Ground Beam Fabrication	Revision A

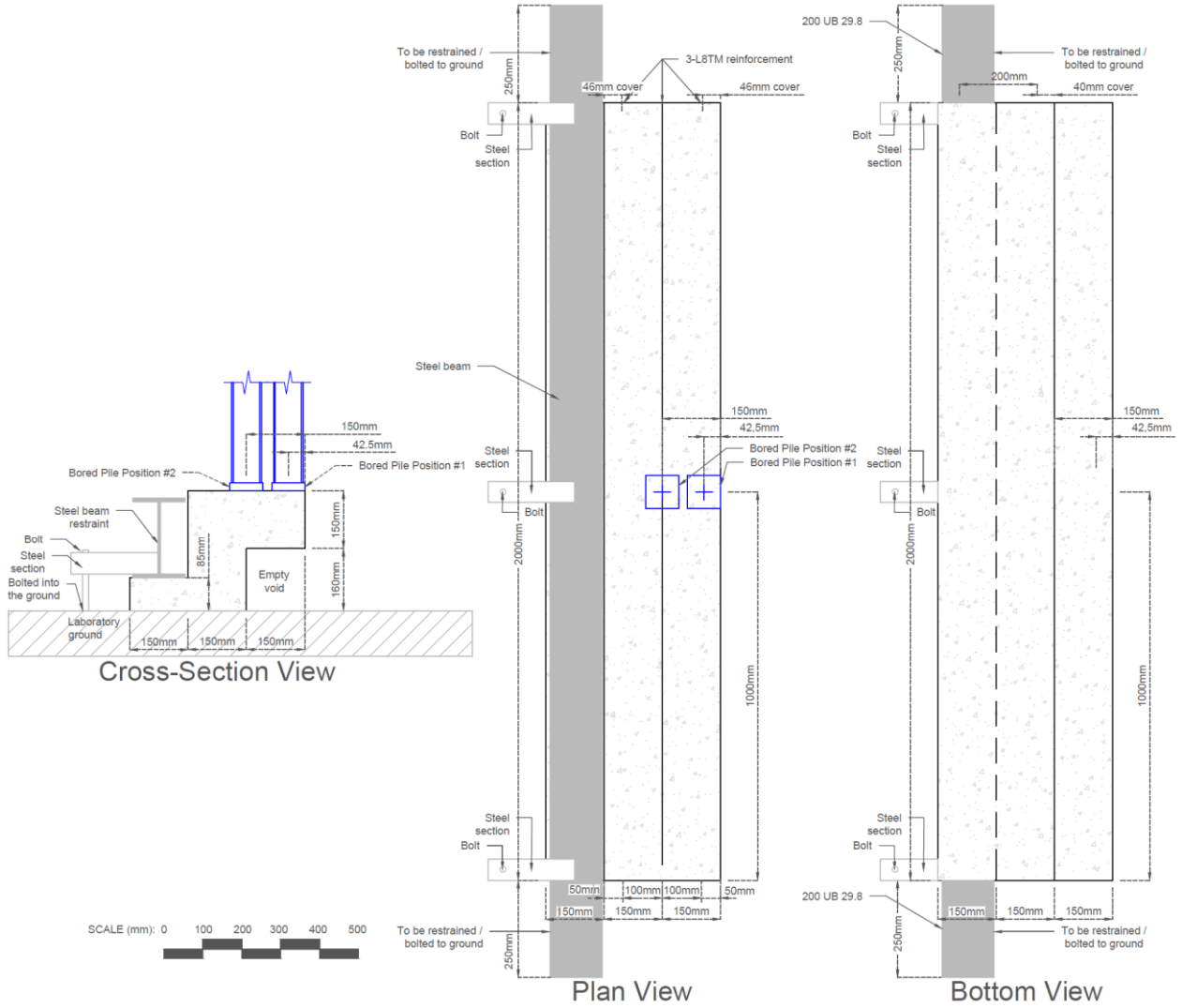

Dwg. 2	Detailed Drawings - Experimental Set-up	Revision A

8.3 Appendix C

8.3.1 Vertical Centroid Calculations

To calculate the vertical centroid, the section was divided into three different shapes, as shown in Figure 32. The datum points for the calculation were specified to be the bottom left corner (0,0). The centroid is then calculated by inputting the specifications summarised in Table 5 into equation (11).

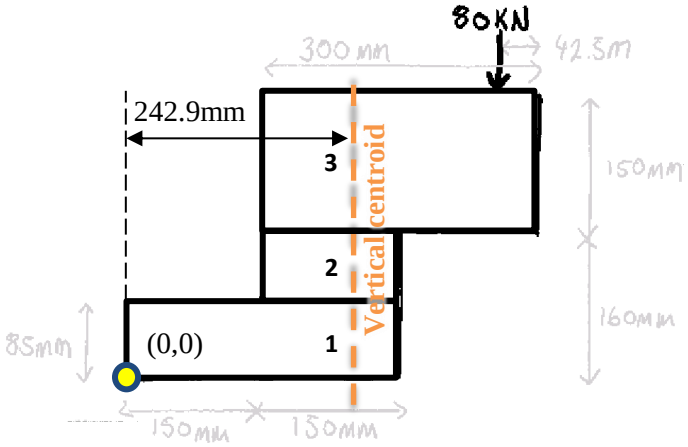

Figure 32. Sectioned Cross-Section of Beam

Table 5. Shape Distance Datum and Areas

Shape number:	**1**	**2**	**3**
Area (mm^2)	25500	11250	45000
Distance from datum (x-direction) (mm)	150	225	300

$$\bar{x} = \frac{\sum x_i A_i}{\sum A} = 242.9mm \tag{11}$$

Hence, the vertical centroid of the section is located at 242.9mm into the beam from the datum.

8.3.2 Moment Balance Calculations

It is known:

- Area of the cross section = 81750mm^2
- Length of the section (L) = 2m,

Therefore, the volume of the concrete beam is 0.1635m^3. Assuming a density of the concrete is approximately 2450kg/m^3, the total estimated weight of the section is 401kg. Thus, the beam will experience a load shy of 4kN. Over the 2m length, the uniform distributed load (w) is 2kN/m. The beam will be lifted from two points, and so the system can be approximated into a simply supported beam with an overhanging section on either side, as shown in Figure **33**.

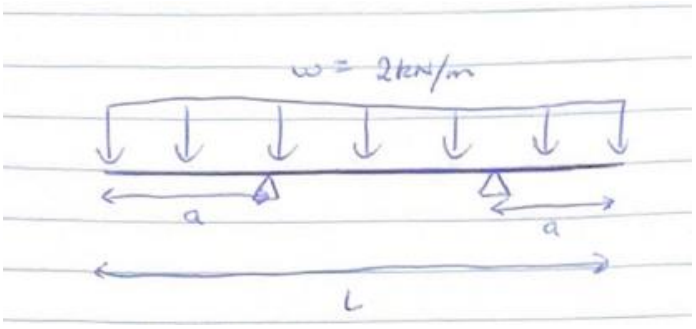

Figure 33. Simply Supported Beam

Substitute L and w into (12):

$$V_{max} = \frac{wL}{2} = 2kN \tag{12}$$

As shown in Figure 34, $M_1 = M_2$, which is given by (13).

$$M_1 = M_2 = \frac{wa^2}{2} \tag{13}$$

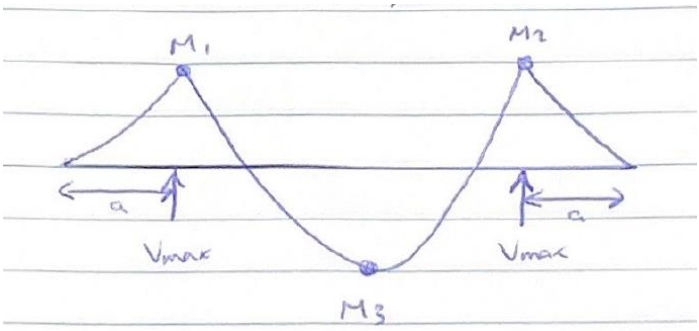

Figure 34. Bending Moment Diagram

Equating M_1 and M_3, and substituting in w = 2kN/m and V_{max} = 2kN into (14) simplifies to (15),

$$M_3 = V_{max} * (\frac{V_{max}}{2w} - a) \tag{14}$$

$$a^2 = 1 - 2a \tag{15}$$

$$\therefore a = 0.41m \; or \; \sout{a = -2.41m} \text{ (cannot be negative)}$$

Thus, the section's moments are balanced when a = 0.41m. Hence for best support, the lifting points should be located 0.41m from the end of the beam.

8.4 Appendix D

8.4.1 Foot Anchor Specifications

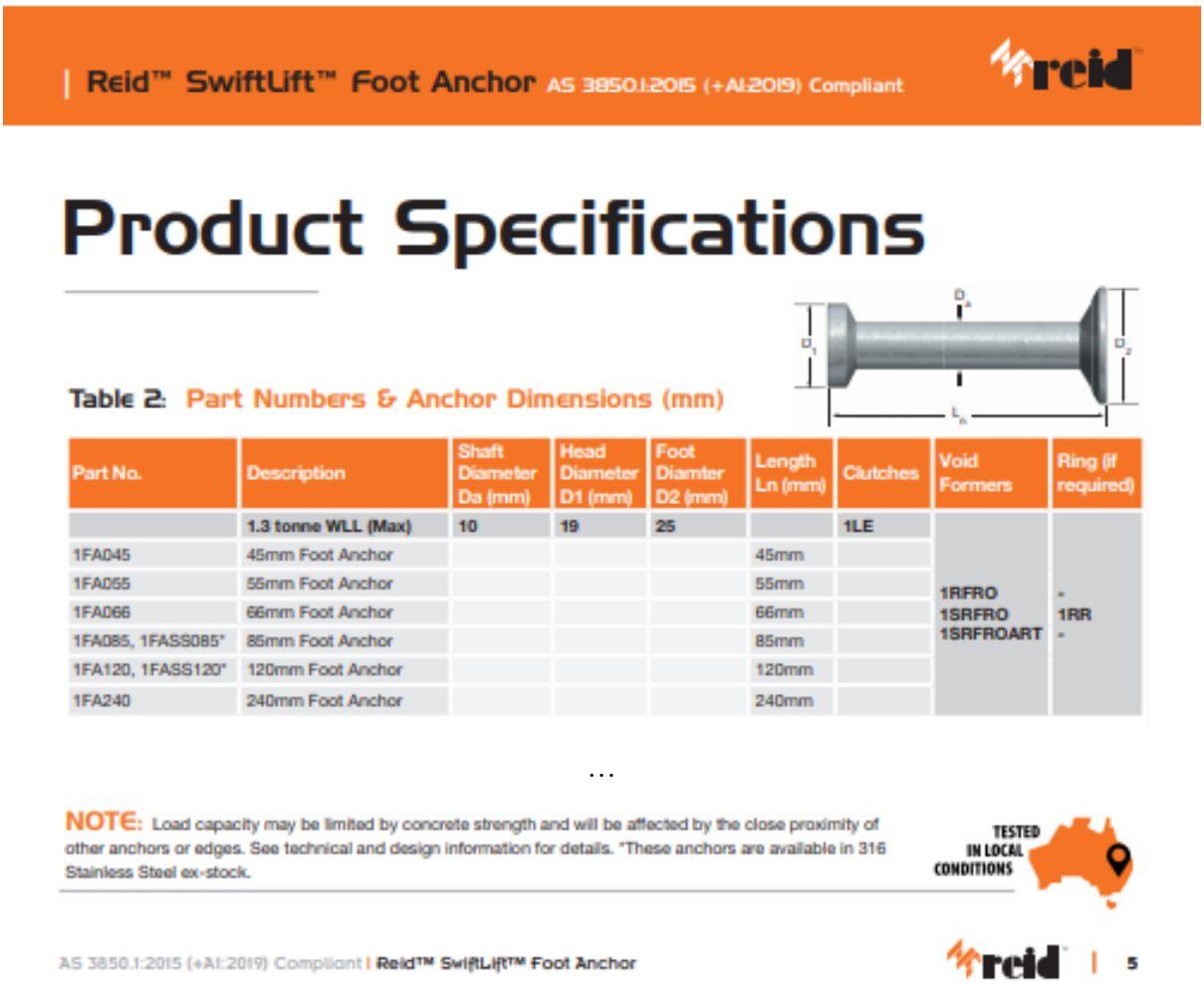

Reid™ SwiftLift™ Foot Anchor AS 3850.1:2015 (+A1:2019) Compliant

Product Specifications

Table 2: Part Numbers & Anchor Dimensions (mm)

Part No.	Description	Shaft Diameter Da (mm)	Head Diameter D1 (mm)	Foot Diamter D2 (mm)	Length Ln (mm)	Clutches	Void Formers	Ring (if required)
	1.3 tonne WLL (Max)	**10**	**19**	**25**		**1LE**		
1FA045	45mm Foot Anchor				45mm			
1FA055	55mm Foot Anchor				55mm		**1RFRO**	-
1FA066	66mm Foot Anchor				66mm		**1SRFRO**	**1RR**
1FA085, 1FASS085*	85mm Foot Anchor				85mm		**1SRFROART**	-
1FA120, 1FASS120*	120mm Foot Anchor				120mm			
1FA240	240mm Foot Anchor				240mm			

…

NOTE: Load capacity may be limited by concrete strength and will be affected by the close proximity of other anchors or edges. See technical and design information for details. *These anchors are available in 316 Stainless Steel ex-stock.

TESTED IN LOCAL CONDITIONS

AS 3850.1:2015 (+A1:2019) Compliant | **Reid™ SwiftLift™ Foot Anchor** | 5

(Ried, 2021)

8.4.2 Breakout failure

The nearest edge is 93mm (c_1) to the proposed lifting location, as shown in Figure 35.

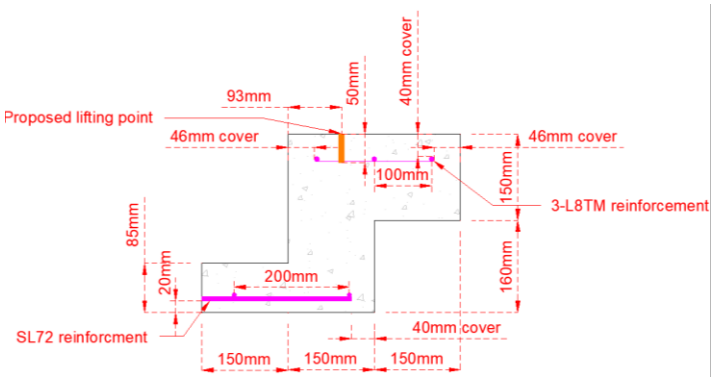

Figure 35. Lifting Location - Cross-Section

The capacity of the selected anchor (Product Code: 1FA045) (outlined in Figure 36) exceeds that experienced during a lift (<4kN).

Part No.	Concrete Compressive Strength, MPa				
	15	20	25	32	40
1FA045	0.8	1.0	1.1	1.2	1.3
1FA055	1.1	1.3	1.3	1.3	1.3

Figure 36. AS 3850.1:2015 (+AI:2019) Tensile and Shear Performance Data (WLL), Tonnes (Ried, 2021)

As c_1>90mm>1.5h_{ef} and the spacing (s_1) >180mm, where the anchor length (h_{ef}) is 45mm, the beam will reach full concrete cone capacity with a breakout area resulting from tensile capacity as shown in Figure **37**.

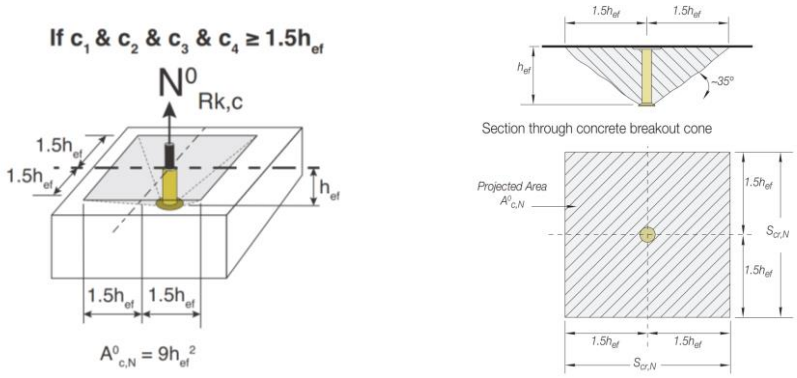

Figure 37. Concrete Breakout (Leviat, 2020)

Therefore, casting recessed 45mm 1.3t rated *SwiftLift™ Foot Anchors* at the proposed locations will be adequate to perform the required beam lifts without concrete breakout failure occurring.

8.5 Appendix E

For the steel beam restraint size to act as an adequate restraint during loading, deflection (δ) due to the applied load must be reasonably small (16).

$$\delta = \frac{PL^3}{48EI} < 5mm \tag{16}$$

Where the applied point load (P) is taken as the maximum capacity of the Katana bored pile ($80kN$), the length of restraining beam (L) is taken as the length of the ground beam ($2.5m$) and Young's Modulus (E) of steel is $200GPa$.

Table 6 shows the range of OneSteel UB sizes considered satisfactory in restraining the ground beam. The beam size width must also be less than or equal to 150mm to fit neatly on the lip of the ground beam.

Table 6. Range of OneSteel UB Sizes Adequate for Restraint Use

OneSteel Designation	Flange width (mm)	Second moment of area (mm^4)	Deflection (mm)
200 UB 29.8	134	29.1e6	4.5
250 UB 25.7	124	35.4e6	3.7
250 UB 31.4	146	44.5e6	3.0
250 UB 37.3	146	55.7e6	2.4

8.6 Appendix F

TEST	DATE	LOCATION	DRIVE NUT/CUT PILE
1	**06/12/21**	**Edge of cantilever**	**Drive nut**
	Not included in report – preliminary test Cast and initial testing - Schmidt hammer only as no cylinders were taken - Significant variation in Schmidt hammer strengths – possibly due to uneven surface - Concrete beam was approx. 5-10mm shy of top of form due to concrete mix not reaching top – resulting in uneven surface - Formwork was not braced, leading to some flex in the centre of the mould Testing - Three I-beams ratchet straps together to load drive nut - Gap between I-beams and drive nut filled by square metal plate - Beam experienced punching shear - Result was lower than expected 64.97kN (54.91kN adjusted) Other notes - Strength – curing time graph analysis		
2	**24/01/22**	**Centre of top section**	**Drive nut**
	Referred to as test 2 in report Cast and initial testing - Cast came out very well - Cylinders tested above expected values 28.13MPa, 220.9kN - Discrepancy between Schmidt hammer and cylinder tests Testing - Mark present for test - Setup flexed considerably during testing – load veered off vertical alignment (actuator not secured in the middle and the steel sections bent under the force) - Beam failed however only exhibited a small crack in the bottom - Didn't fail via punching shear as many of the other beams did, failed via flexure 264.04kN (223.13kN adjusted) Other notes - Beam to be used again in a different test (test 4) - Need to modify testing setup so there's less bending in the actuator/steel sections		
3	**31/01/22**	**Between edge and centre**	**Drive nut**
	Referred to as test 3 in report Cast and initial testing - Cylinders tested above expected values 26.27MPa, 206.3kN Testing - Used CLT instead of steel sections for this test - Far less flex experienced - Crack exhibited at 66.52kN - Continued testing and reached 111.94kN (97.67kN adjusted)		

<table>
<tr><td></td><td colspan="3">Other notes
Graph plotting of theoretical and practical results
- Find some sort of relationship (if possible)
- Extrapolate maximum position from edge that satisfies axial force requirements before failure.</td></tr>
<tr><td>4</td><td>18/02/22</td><td>Centre of top section</td><td>Cut pile</td></tr>
<tr><td></td><td colspan="3">Referred to as test 4 in report -
Cast and initial testing
- Cast came out well
- Top surface smooth and flat
- Cylinders exhibited large strength variation (16.89, 15.28, 11.05MPa)
- Postponed testing by a day to allow concrete to strengthen more
- Cylinders exhibited large strength variation (16
Testing
- New testing setup using a piece of CLT worked well
- Testing adjusted halfway through (step shown in testing graph)
- Cut pile used
- Failed via punching shear, caused by local crushing
- Tested above expected value
161.73kN, 133.9kN (adjusted)
Other notes
- Only cut pile test performed
- Tilting setup may help cause punching shear</td></tr>
<tr><td>5</td><td>11/04/22</td><td>Edge of cantilever</td><td>Drive nut</td></tr>
<tr><td></td><td colspan="3">Referred to as test 1 in report
Cast and initial testing
- Top of beam a little rough, not as smooth as previous pours
- Drive nut partially cast into top section of beam to ensure a flat surface
- Cylinders tested below expected values on day 14
- Irregularities within cylinders
Testing
- Failed via punching shear</td></tr>
</table>